CALVAL ERS
CLS.DOS/NT/06.001
Version : 1rev1, January 28th 2006
Nomenclature :

Ramonville, January 28th 2006

ERS-2 OPR data quality assessment
Long-term monitoring - particular investigation

Annual report 2005 of IFREMER Contract No 05/2.210 166

	AUTHORS	COMPANY	DATE	INITIALS
WRITTEN BY	F. MERTZ	CLS		
	F. MERCIER	CLS		
	S. LABROUE	CLS		
	N. TRAN	CLS		
	J. DORANDEU	CLS		
APPROVED BY	J. DORANDEU	CLS		
QUALITY VISA	M. DESTOUESSE	CLS		
APPLICATION AUTHORISED BY	J.-F. PIOLLE	IFREMER		

DISTRIBUTION LIST

COMPANY	NAMES	COPIES
CLS	F. MERTZ	1
CLS	F. MERCIER	1
CLS	S. LABROUE	1
CLS	N. TRAN	1
CLS	J. DORANDEU	1
CLS	M. DESTOUESSE	1
IFREMER	J.-F. PIOLLE	1
IFREMER	B. CHAPRON	1

CHRONOLOGY ISSUE

Control Initials	ISSUE	DATE	REASON FOR CHANGE
	1rev1	28/01/2006	Creation

List of Tables

List of Figures

Contents

1 Introduction

The ERS-2 satellite was successfully launched in April 1995 and has flown all over the globe during 8 years in a 35-day repeat cycle mission. On June 2003 (during cycle 85), the on-board register failed, impacting the delivery of the data on the global coverage. Indeed, since the end of cycle 85, the data are available within the visibility of ESA ground stations over Europe, North Atlantic, the Arctic and western North America. Nevertheless, long-term monitoring can be carried on for the main altimeter and radiometer parameters, and this is one of the goals of this work. With the availability of Envisat on the same ground track as ERS-2, the long time series which begun with ERS-1 is going to grow. To provide oceanographers with high quality data, it is necessary to get as best as possible ERS-2 data to mix with Envisat. This is the reason why in the last year report many recommendations were made to improve the quality of ERS-2 data.

One of the purpose of this report is to carry on with the study of the non parametric SSB. The use of new corrections and new orbit in the computation of the SSH imposed to fit a new SSB estimate. Prior to this estimation, it has been useful to focus on the methodology used in the estimation. This work is presented in the second part of the present report.

Thanks to ERS-2 data particularly, much progress has been made on the understanding of the Ocean. But there are still a lot to learn from the data. Indeed, it is a new challenge in altimetry to try to improve the data quality in coastal regions and then to be involved in many studies that are linked to such thematic. The last part of this study deals with the computation of available altimetric measurements near the coast. A wet troposphere correction is proposed, combining radiometer and model wet troposphere when possible to enhance the quality of the data near the coast. Then, a mean profile is computed and is compared to the one usually used.

2 Long-term monitoring of altimeter and radiometer parameters

2.1 Data used

ERS-2 OPR cycles 1 to 108 (from May 1995 to September 2005) have been processed until the end of year 2005. The OPRs have been distributed by the CERSAT centre, and are described in the CERSAT User Manual, 1996 [2]. All the corrections given in the Quality Assessment Reports (Mertz et al, 2005, [18]) are applied.

The summary of the general events that occured on the ERS-2 mission was made in the previous ERS-2 annual report (Mertz et al., 2004, [17]. On June 2003 (during cycle 85), the on-board register failed, impacting the delivery of the data on the global coverage. Indeed, since the end of cycle 85, the data are available within the visibility of ESA ground stations over Europe, North Atlantic, the Arctic and western North America. The figure 1 is the number of valid points for each cycle.

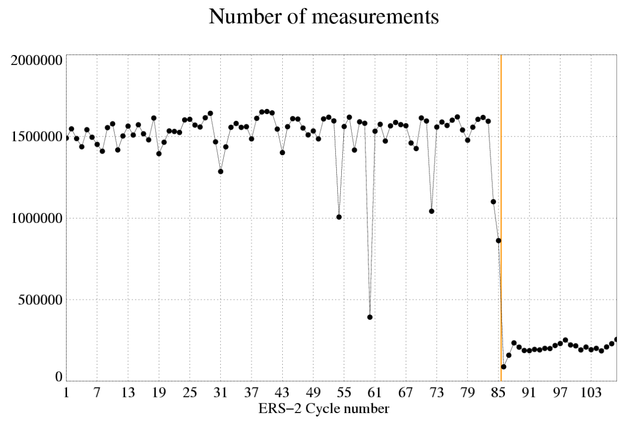

Figure 1: *Number of edited measurements for cycles 1 to 98*

2.2 Mispointing

Since cycle 60 (January 2001), the version 6.5 of OIP processing computes the 1-Hz estimate and the smoothed estimate of the waveform-derived square of the off-nadir angle (mispointing) as described in Van Den Bossche and Zanife, 2001 [23]. The mispointing is useful to notice problems in the platform attitude control. Histograms and statistics are computed on every cycle for ascending and descending passes from cycle 61. The values of the mean and standard deviation for ascending and descending passes are reported on figure 2. The failure of the Digital Earth Sensor (January 2001, cycle 60) leaded to a degradation of the attitude control during cycles 61 and 62. An annual signal is evidenced for the mean descending passes and more strongly for the mean and standard deviation on ascending passes. This signal may be increased by some platform events such as the upload of the upgraded version of attitude control on November 28th 2001 (cycle 69), and the switch off of the ERS-2 payload in March 2002 (cycle 72). The low mean value (less than 0.1 degree) and stable value of the standard deviation indicate an improvement in the attitude control quality. The negative value of the mean is probably due to the use of the same IF filter in the OPR processing throughout the whole ERS 2 mission (Van Den Bossche and Zanife, 2001 [24]). We can note that the values for the standard deviation from cycle 86 onwards increase, as expected, because of the restricted area. Nevertheless, except the higher values for cycles 88 to 92, no clear impact is visible on the mean.

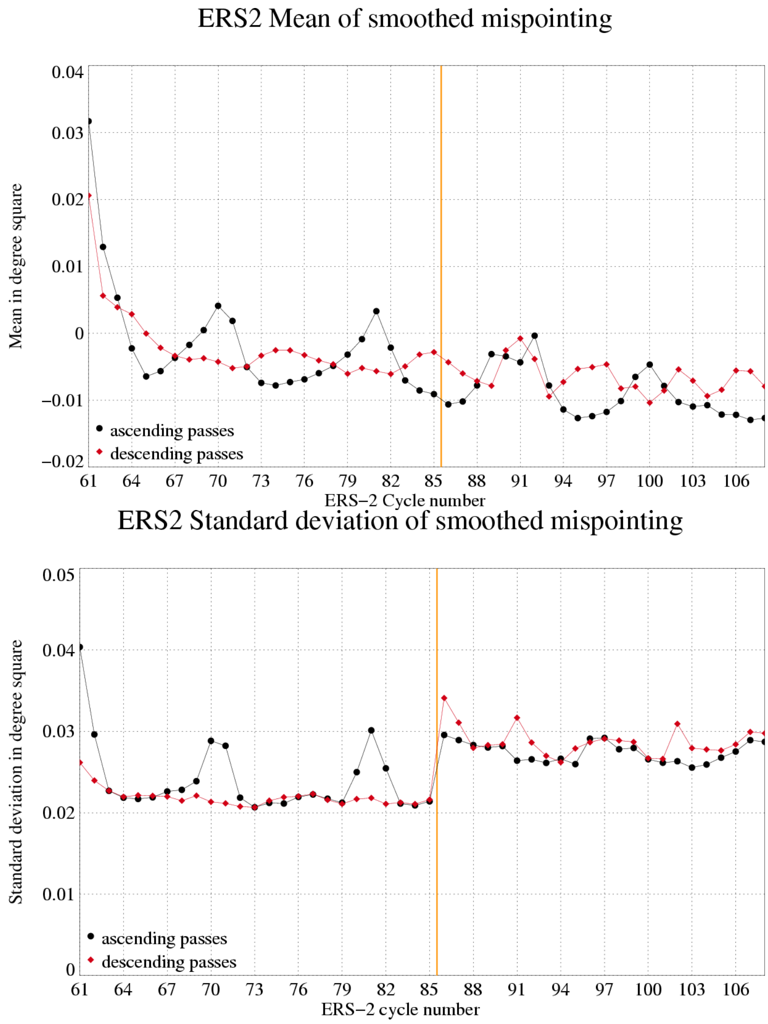

Figure 2: *Cycle mean (top) and standard deviation (bottom) of mispointing for ascending and descending passes.*

2.3 Backscatter coefficient

For the present long-term monitoring of the backscatter coefficient, correction of the OPR backscatter coefficient has been applied using the values reported in Dorandeu et al., 2000 [3], who studied the impact of the ERS-2 platform attitude control degradation in the beginning of year 2000. The mean, median, standard deviation and skewness are computed for each cycle. The backscatter coefficient value corresponding to the peak of the histogram, as well as the percentage of samples in the peak bin and in the median bin are also computed, to detect a possible modification of the histogram shape with time (figure 3). The values of the statistics after cycle 86 are more sensitive to the seasonal signal than before due to the reduction of the geographical coverage and hence, the number of data. The values of the mean, median, standard deviation and skewness are relatively stable until cycle 85. The curve of the maximum sampling values is close to the one of median values until cycle 50, and it is close to the curve of mean values onwards. This corresponds to the change of the shape of the histogram revealing 2 main peaks in the distribution. The lower values of this latter parameter for some cycles indicates a raise of the secondary peak on the left of the main peak. This is corroborated by the decrease of the percentage of points in the maximum sampling and median bins (figure 3 bottom).

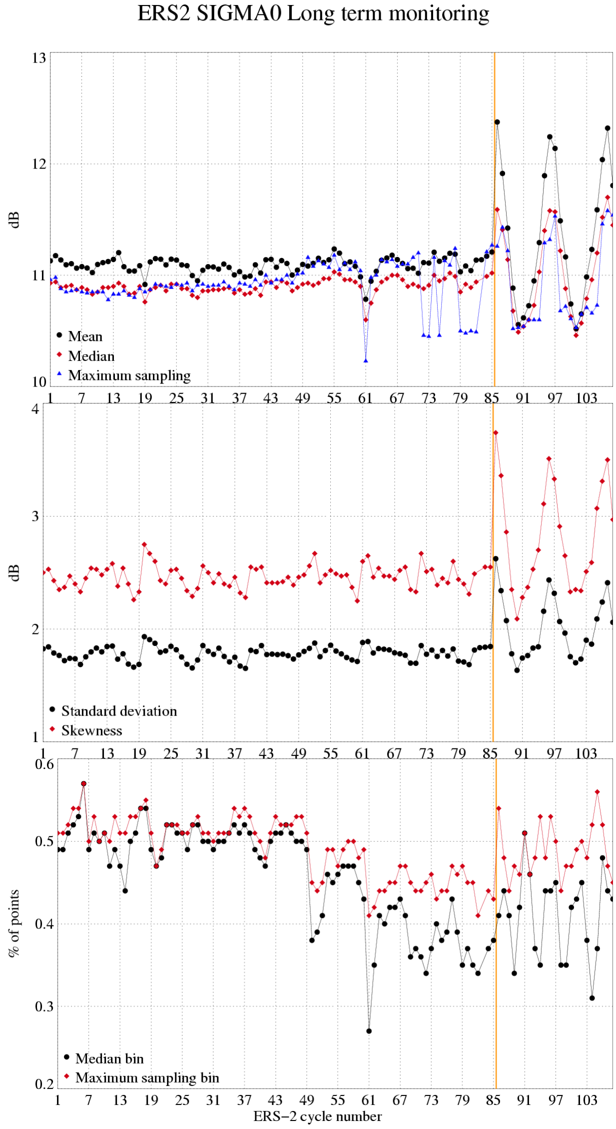

Figure 3: *Statistical results on the ERS-2 OPR backscatter coefficient*

2.4 Significant wave height

The same statistics as SIGMA0 are computed (figure 4). The percentage of points in the 0-values bin is also reported on the bottom plot. For the period from May 95 to June 2003, the statistics are very steady with a seasonal signal on the standard deviation and the percentage of points in the 0-values bin. For the period after cycle 85, the seasonal signal is amplified and visible on all the parameters. This implies in particular that the number of 0-values is at maximum over summer cycles as shown on the top chart of the figure. An example of the histograms is shown on figure 5 for which the number of points is about 600 for the mean values of SWH but in cycle 86, the number of 0-values is more than 1100 and it is lower than 200 for cycle 91.

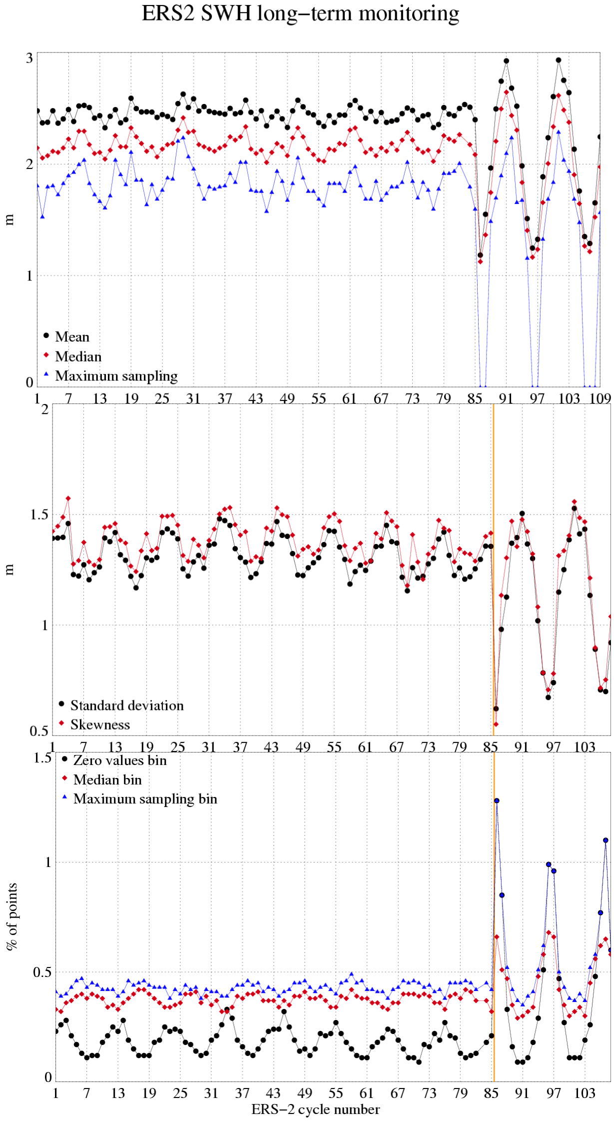

Figure 4: *Statistical results on the ERS-2 OPR significant wave height*

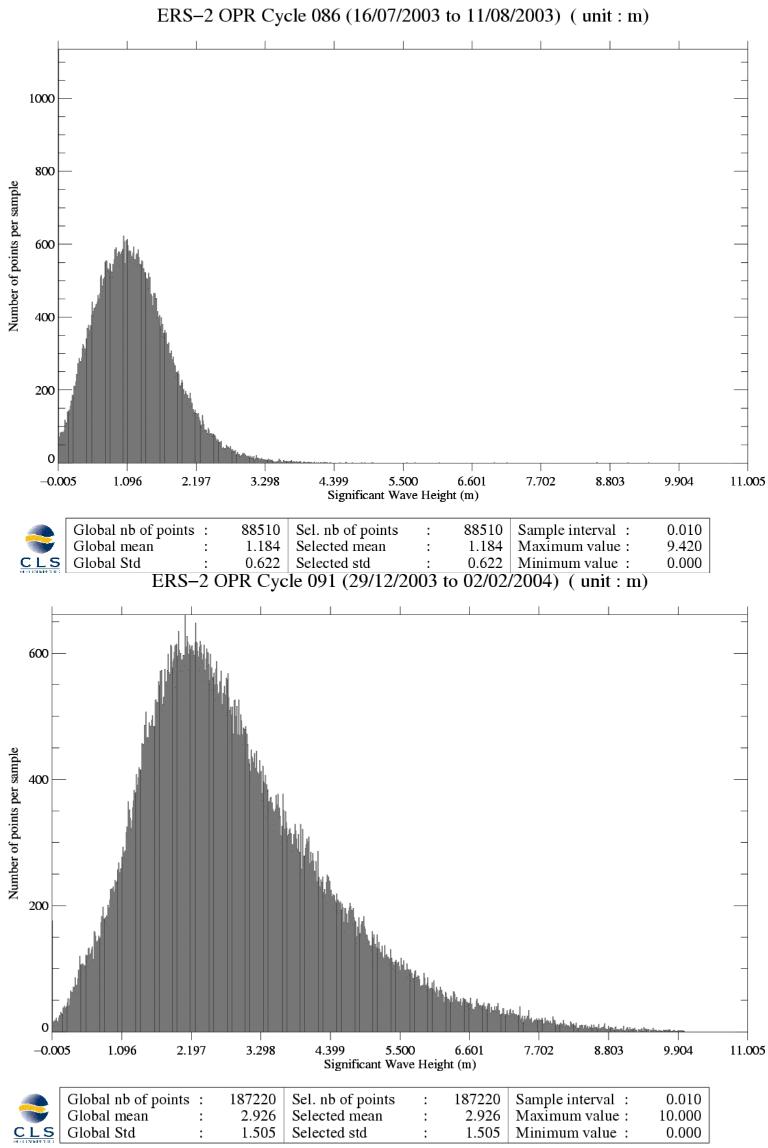

Figure 5: *Histograms of the ERS-2 OPR significant wave height for cycles 86 and 91*

2.5 Radiometer parameters

The mean and the standard deviation of difference of (ERS-2-ECMWF) wet troposphere corrections (WTC) are monitored since the beginning of the mission (figure 6). The standard deviation of the difference decreases gradually, corresponding to improvements of the ECMWF model. This is also observed in time series of (ECMWF-TOPEX) differences (Ablain, 2005 [1]). For the mean values, two computations have been reported, one with the correction of the drift given by Eymard et al., 2003 [7] (called mean with EAL) and ont with the correction given by Scharroo et al.,2004 [20] (call mean with SAL). This new correction clearly impacts the values after the gain fall (cycle 12) and in the long term, after cycle 60, with a difference with the previous value of about 4 mm at cycle 85. This last correction was one of the recommendations made in the last annual report.

The improvements of the model are evidenced on the chart:

- since December 1$^{\text{th}}$, 1997 (middle of cycle 27), the quality of the model has been improved, after correction of an error in the French Met Office Software. The data provided before cycle 27 are then corrected (Mertz et al., 2004 [18]) afterwards as follows :

  $$\text{ModelWTC}_{\text{corrected}} = 0.85\text{ModelWTC} + 6$$

  where WTC is taken positive and is in mm.

- Another improvement of the model is observed at cycle 70 in January 2002 (ECMWF [5]).

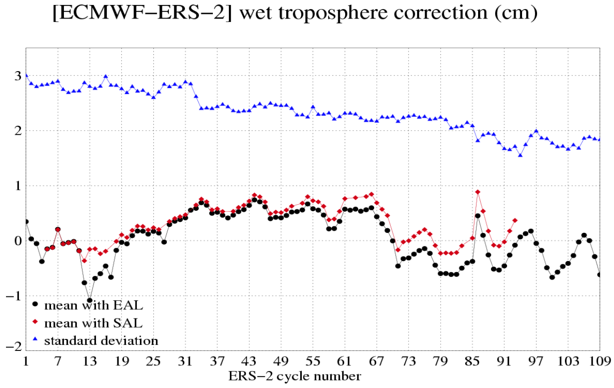

Figure 6: *Mean and standard deviation of (ECMWF - ERS-2) wet troposphere correction*

2.5.1 Estimations of biases on brightness temperatures

2.5.1.1 Introduction

A recent algorithm has been included in the Envisat GDRs to compute the radiometer wet troposphere correction. It is based on neural network technique and is described in Labroue and Obligis, 2001 [13]. Such algorithm has been applied to ERS-2 data as explained by Tran, 2003 [21] and was tested during year 2004 (Mertz et al., 2004 [17]). Significant improvement is obtained particularly in dry regions. The neural algorithm was estimated for Envisat measurements based on data from ECMWF model. Then, biases were computed between Envisat and ERS-2 to have algorithms input as similar as possible between the two instruments. Those biases were obtained over only one cycle to compute the gap between the two altimeters. The aim of this study is to compute a new set of biases on the basis of one year of data in order to get rid of annual signal and lack of data. Indeed, it was proposed this year to apply to ERS-2 the new estimation made for Envisat using improved ECMWF model fields but this correction is not available yet for Envisat. Nevertheless, it is possible to estimate the bias between the TBs. A drift was detected in Envisat TB 36 GHz parameter and Tran et al., 2005 [22] recently proposed a correction.

2.5.1.2 Long-term monitoring

Before to provide a statistical value for the biases, a monitoring of the radiometer parameters has been performed. Figure 7 shows the cycle mean difference of (ERS-2-Envisat) TBs over the whole Envisat mission. This is part of the work done by the cross-calibration of Envisat and ERS-2. The ERS-2 TB 23.8 GHz have been corrected for the Eymard drift (Eymard et al., 2003, [7]) called EAL and for the drift proposed by Scharroo et al., 2004 [20] called SAL. For TB36.5 GHz Envisat, the results are shown with and without the correction of the drift proposed by Tran et al., 2005 [22]. The differences are calculated for each collocated point of both satellites. This implies that after cycle 17, the geographical area is much restricted, due to the failure of the LBR recorder on ERS-2 in June 2003.
The behaviour of the differences are thus different for cycles before cycle 17 and after. A seasonal signal is visible for the period before June 2003 and it is less

marked after, mainly on the TB 36.5 GHz differences. The TBs differences will be further discussed in the Envisat yearly report Faugère et al., 2005 [8].

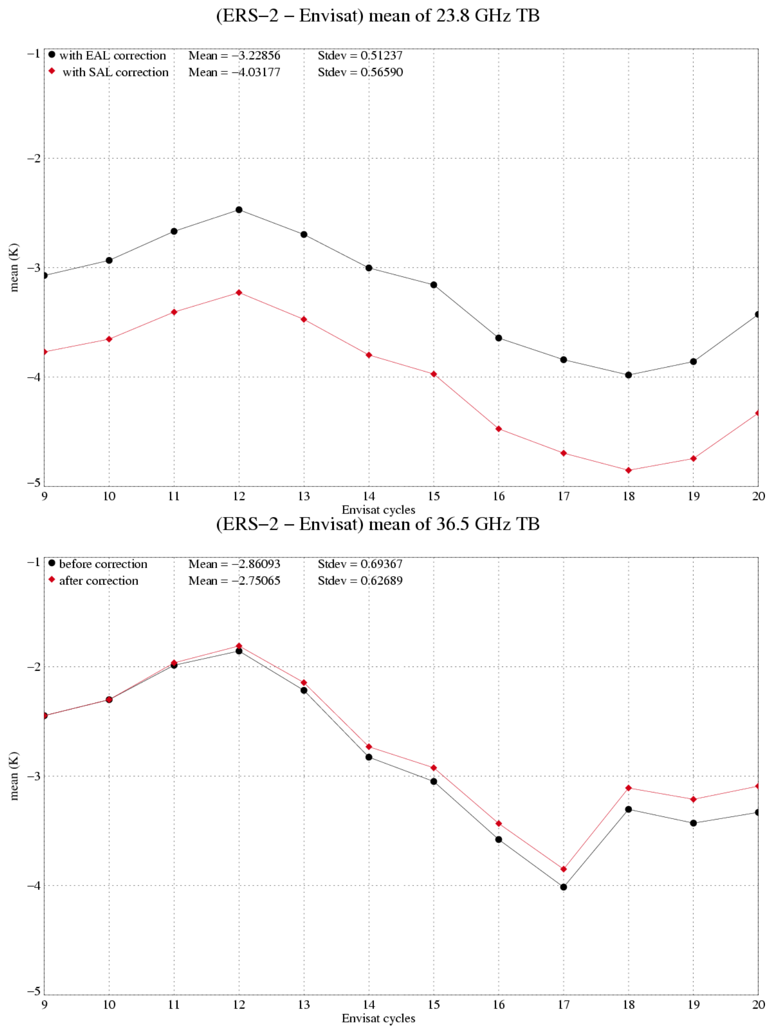

Figure 7: *Mean of (ERS-2 - Envisat) TB 23.8 GHz(top) and TB36.5 GHz(bottom)*

2.5.1.3 Computation of the biases

Table 1 provides the biases between ERS-2 and Envisat for Envisat cycles 9 to 20. The ERS-2 TB 23.8 GHz have been corrected for the drift proposed by EAL and by SAL. The last column shows the difference in channel 36.5 GHz taking into account the drift proposed by Tran et al., 2005 [22]. Considering cycles 9 to 20, the weighted mean values are -2.99K with EAL and -3.77K with SAL for TB23.8 and -2.52 K for TB36.5. Those values differ up to 0.02 K when considering a smaller period (cycles 9 to 17) with a whole geographical coverage. The bias obtained TB 23.8 GHz is close to the one obtained by Tran, 2003, which took into account cycle 10 only.
Regading TB 36.5 GHz, the value differ by 0.13 K from the one obtained by Tran. It is not surprising given the large signal obtained for the first 10 cycles, with a difference of -2.14 down to -3.85 between cycles 13 and 17.

Cycle	Number of points	TB 23.8 GHz(K) (EAL)	TB 23.8 GHz(K) (SAL)	TB 36.5 GHz(K)	TB 36.5 GHz(K) (EN corrected)
9	36515	-3.0710	-3.76878	-2.4466	-2.4466
10	130719	-2.9328	-3.65236	-2.3005	-2.3005
11	203196	-2.6672	-3.40489	-1.9862	-1.9638
12	212037	-2.4701	-3.22699	-1.8559	-1.8094
13	199194	-2.6961	-3.47195	-2.2155	-2.1444
14	162036	-3.0019	-3.7971	-2.8258	-2.7304
15	110832	-3.1566	-3.97145	-3.0479	-2.9226
16	121397	-3.6420	-4.47192	-3.5780	-3.4319
17	112385	-3.8405	-4.69415	-4.0133	-3.8492
18	11001	-3.9803	-4.85062	-3.3024	-3.1076
19	18434	-3.8574	-4.74324	-3.4284	-3.2106
20	30597	-3.4261	-4.3278	-3.3301	-3.0901

Table 1: *Biases and correction to apply to ERS2 data*

2.6 Sea surface height

The corrections used to compute the SSH for ERS-2 is given in the next table:

Parameter	From product or updated	Algorithms
Orbit	Updated	DGME-04 (Scharroo and Visser, 1998 [20])
Range	From product and corrected	SPTR2000 (Martini and Féménias, 2000 [16])+ USO drift + Time Tag Bias
Ionosphere correction	From product and updated	BENT (cycle before 50) and GIM (cycle after 50)
Dry troposphere correction	Updated	Model dry tropospheric correction computed from rectangular grids (new S1 and S2 atmospheric tides are applied)
Inverted Barometer	Updated	Combined atmospheric correction : MOG2D and inverse barometer computed from rectangular grids
Radiometer wet troposphere	Corrected	Gain fall correction + TB Drift (Scharroo et al., 2004 [20])
Sea State Bias	Updated	BM3 (Gaspar and Ogor, 1996 [10])
Ocean and loading tide	Updated	GOT 2000 (S1 and S2 included)
Terrestrial tide	From product	
Polar tide	Updated	
MSS	Updated	CLS 01 Mean Sea Surface

Table 2: *SLA formula for the long-term monitoring*

The results are plotted on figure 8. Regions of high oceanic variability (30 cm) and of shallow waters (<1000 m) have been removed. The statistics are calculated with GIM [12] ionosphere correction after cycle 50. Nevertheless, the mean for cycles 75 to 85 seems to be higher than expected, including a trend in the global curve. However, the strong solar activity may also have impacted the orbit precision (observed for instance in cycle 68, during a geomagnetic storm), and led to increase the standard deviation.

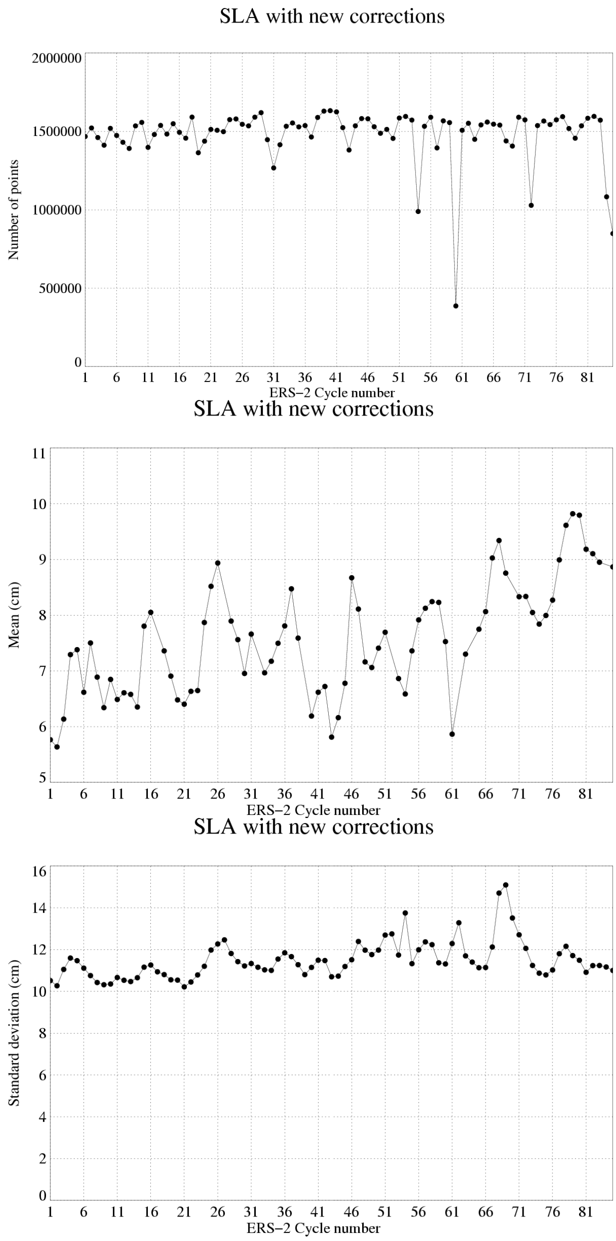

Figure 8: *Cyclic number of points (top) mean (middle) and standard deviation (bottom) of SLA with new corrections applied*

2.7 Conclusion

The variation with time of the OPR Altimeter data quality has been examined using statistical analysis performed on the main OPR parameters.

- Instrument problems caused mispointing in cycles 60 to 63 and 69 to 72, leading to some degradation of the altimeter parameters (main impact on backscatter coefficient).
- The ERS-2 backscatter coefficient experienced a series of (small) jumps at the beginning of year 2000, part of which are due to the platform attitude control degradation. Since cycle 50, the shape of the histogram has changed and has never recovered, contrarily to the mean.
- There is no evidence of significant wave height degradation or trend over time.
- The ionosphere correction has a strong impact in the SSH monitoring, and it is preferable to use GIM algorithm. The drawback is that no model is provided before cycle 50.
- Biases have been computed between Envisat and ERS-2 TBs taking into account one year of data and the up-to-date corrections of the respective drifts: the one proposed by Scharro et al., 2004 [20] for ERS-2 TB23.8 and the one proposed by Tran, 2005 [22] for the Envisat TB36.5. This will allow to apply to ERS-2, the new Neural Network algorithm (which might be proposed during year 2006) for Envisat.
- Due to statistics over restricted area, the results are noisier from cycle 86 onwards. Given the two years of monitoring from cycle 85, the seasonal signal is clearly evidenced and amplified compared to the previous period. All the statistics are impacted. It is unfortunate that the coverage over this restricted area is not full and that a lack of data in the middle of North Atlantic Ocean still remains.

3 Non parametric SSB estimation

3.1 Introduction

A non parametric (NP) SSB estimation was performed last year on ERS-2 data (Mertz et al., 2004 [17]). It was the first time that this technique was applied on this altimeter. Indeed, the SSB given in the OPRs is -5.5% of SWH, which is a simple estimation of the correction and the SSB recommended to the users at this date on ERS-2 data is the one computed by Gaspar and Ogor in 1996 [10] and is called BM3. It has been estimated by fitting a three-parameter SSB model from SSH crossovers. In the previous study, one year of data was taken into account with the aim to compare the contribution of the ionosphere and the orbit error correction in the estimation. The calculation of the SSB was performed with the three existing methods (crossovers, residuals and direct) and it appeared that the residuals method gave the best estimate in terms of statistics.
During the year 2005, many improved geophysical corrections have been included in the processing of the new generation of altimeters and some of them are described in the last annual report [17]. Obviously, the SSB estimation for ERS-2 has to be fitted with this new generation of SSH to be homogeneous with the other altimeters and to be proposed in a potential reprocessing. This is what is proposed in this study.
Previously, a refinement of the input crossover data set to the SSB estimate is performed. The impact of the new Delft orbit (EIGEN-GRACE) is also analysed. Finally, estimates from collinear differences and direct method are computed and they are compared to the crossover estimate by the statistical method.
The 10 last complete cycles of ERS-2 are taken into account in the present study, with the aim to allow comparisons between ERS-2 and Envisat SSB estimate.

3.2 Spline interpolation and window parameters

In the last study [17], a test was performed in the estimation process by increasing the smoothing window in the wind speed direction. This allowed to extend the availability of the estimation and to smooth the estimations. Some work has been performed this year to get a good compromise between the window parameters and the input data at crossovers. Indeed, the characteristics of the SSH and SWH data are better taken into account using a spline filtering of noise 6 cm for SSH and 40 cm for SWH in the calculation of the crossovers. The usual value for Envisat are 3 cm and 20 cm respectively. This computation allows to take into account the values obtained for ERS-2 of the standard deviation of the 20-Hz range and SWH measurements which are twice higher than for Envisat. A SSB estimation has been carried out with a smoothing window of (3m/s,1.5m) and is presented in figure 9. The impact of splines filtering on the estimations is given in figure 10. SWH gradients are found for SWH below 4m and wind speed gradients are found for values above 18m/s, indicating lower values with spline filtering. This allows to smooth the the estimations in regions of low SWH. With the window of (3m/s,1.5m), the region of SWH between 4 and 6 m and low wind speed gives estimations with higher gradients than for lower SWH but it is very respectable. Thanks to the work done by Labroue et al., 2005 [15], a method has been developed to calculate estimation for each SWH and U of the definition set. This method will be applied later in this study in the last step of the global SSB estimation.

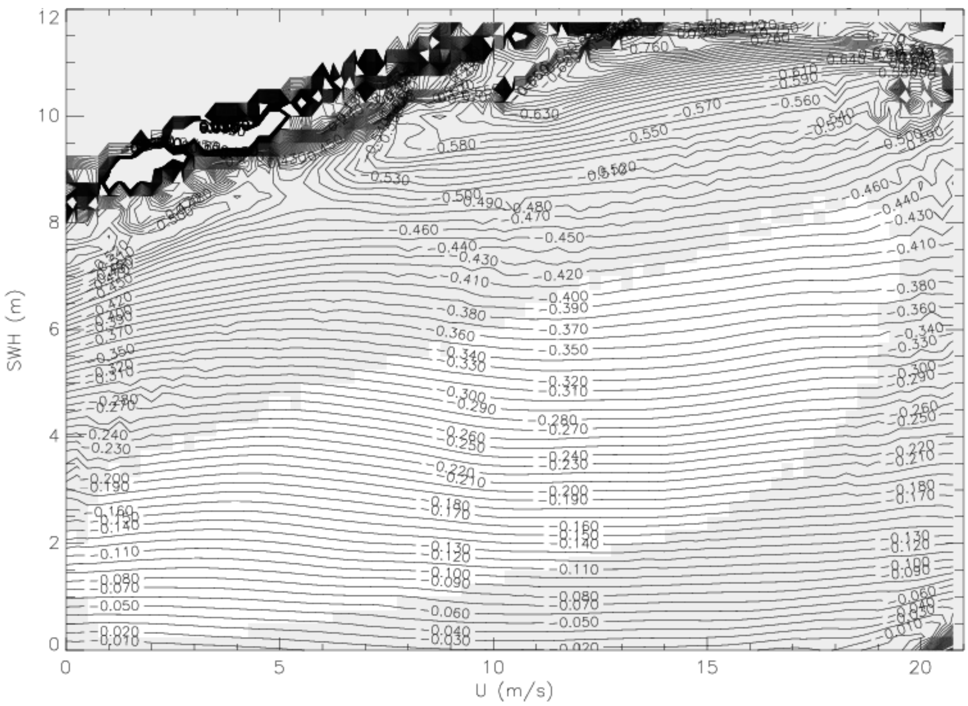

Figure 9: *SSB estimation with spline interpolation and (3m/s,1.5m) window parameter*

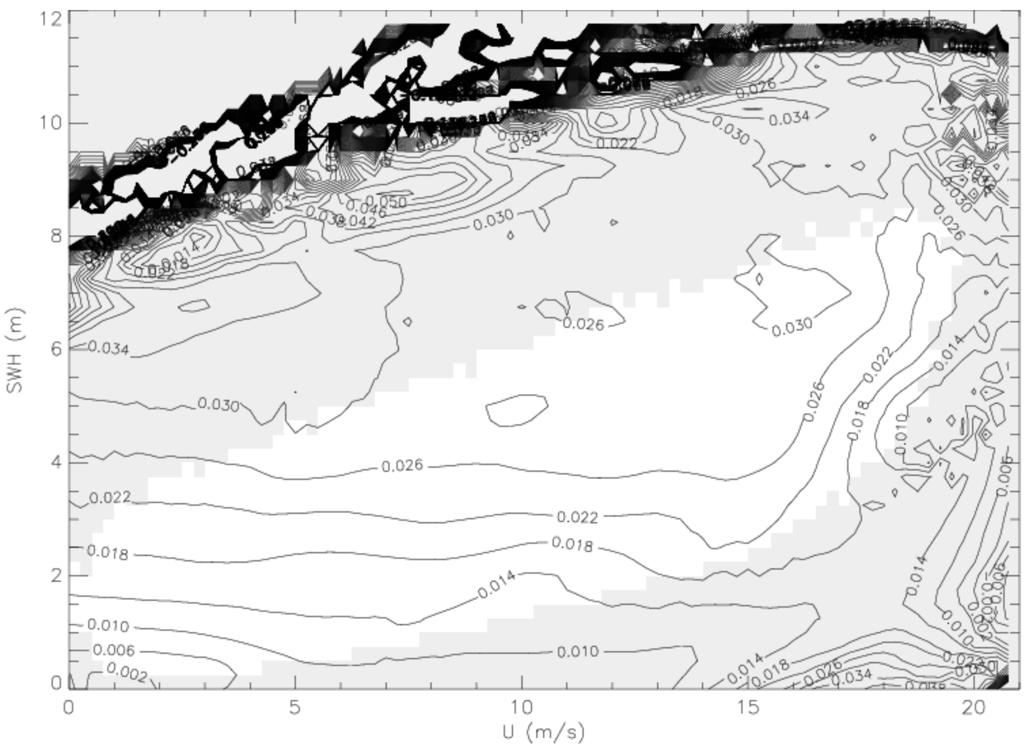

Figure 10: *Difference of SSB estimate with and without spline filtering*

3.3 Estimation with new SSH and EIGEN-GRACE01S orbit

The crossovers were formed by smoothing both the raw SSH and SWH by splines. The crossovers between -66 and 66 degrees and a time lag less than 10 days have been selected.
The EIGEN-GRACE01S orbit provided by Doornbos and Scharroo from the Delft University has been used [4]. Enhanced gravitational and non-gravitational force models are used to maintain the best attainable orbit accuracy. A prior estimation of the datation bias has been estimated on the orbits. It comes out that the coefficient obtained by a regression analysis is equal to 1.06 ms for EIGEN-GRACE01S orbit and 0.95 ms for DGME-04 over the considered period. This correction was applied systematically on the SSH instead of the 1.1ms usually used. The SSH formula used for this estimation is described in table 3. In particular the atmospheric components are better applied than before with the use of MOG2D and the new Inverse Barometer. Moreover, the S1 and S2 components are correctly computed in the tidal and dry troposphere corrections.
The resulting SSB estimation is given in figure 11. The values are about -12 cm for mean sea state conditions and can reach -40 cm for strong sea state conditions. The estimations are very regular even with higher wind speed boarder and below 4m. For low wind speed higher gradients appear for SWH above 3.5 m.

Parameter	From product or updated	Algorithms
Orbit	Updated	EIGEN-GRACE orbit delivered by Delft [4]
Range	From product and corrected	SPTR2000 (Martini and Féménias, 2000 [16]) + USO drift + current Time Tag Bias
Dry troposphere correction	Updated	Model dry tropospheric correction computed from rectangular grids (new S1 and S2 atmospheric tides are applied)
Inverted Barometer	Updated	Combined atmospheric correction : MOG2D and inverse barometer computed from rectangular grids
Ionosphere correction	Updated	GIM model
Wet troposphere correction	From product	ECMWF model
Ocean and loading tide	Updated	GOT 2000 (S1 and S2 included)
Terrestrial tide	From product	
Polar tide	Updated	

Table 3: *SSH formula for SSB study*

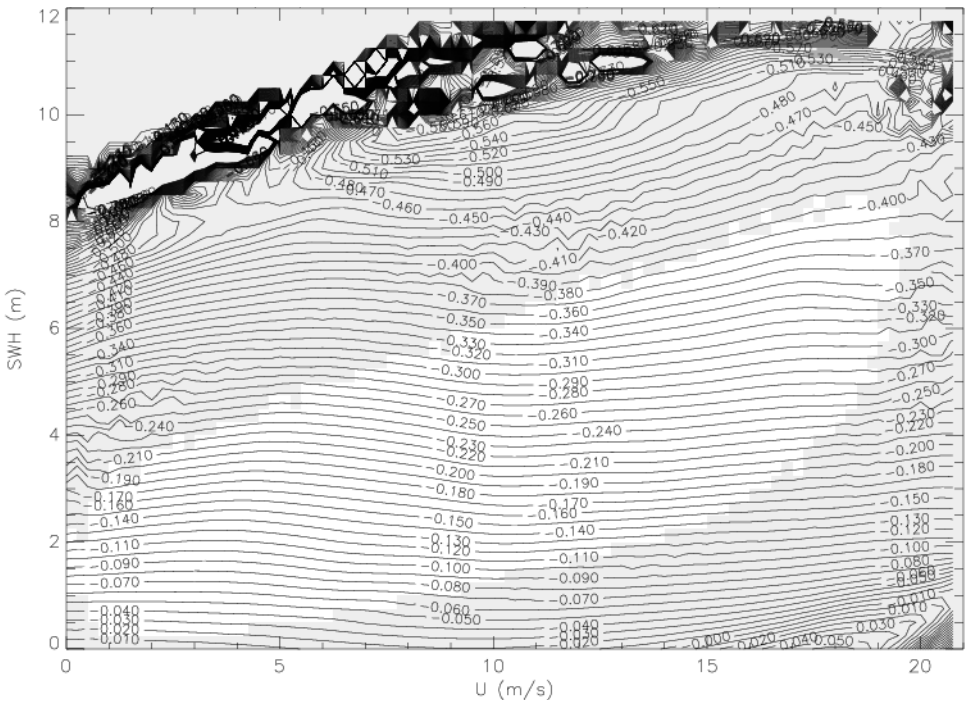

Figure 11: *SSB estimation using EIGEN-GRACE01S orbit and new corrections in SSH*

3.4 Impact of corrections used in SSH

Some of the recommendations of the last annual report (Mertz et al., 2004 [17]) have been taken into account as described in table 3. There are the atmospheric correction combining MOG2D barotropic model and Inverse Barometer, the GIM model ionospheric correction. Moreover, the S1 and S2 components of the atmospheric tides are corrected in the right way. The crossover SSH differences are plotted on figure 12 with the "old" corrections (top) and with the "new" corrections (bottom). The main difference between the two maps is located in the Indian Ocean. This is mainly explained by the use of the corrected S2 signal. The impact of MOG2D model is visible along the equator, mainly in Pacific Ocean. There is still a strong hemispheric signal and a particular behaviour in the tropical Atlantic attributed to GIM ionosphere correction.

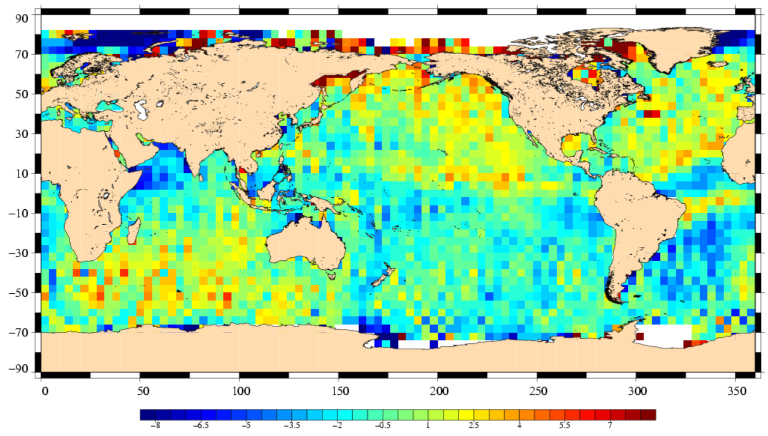

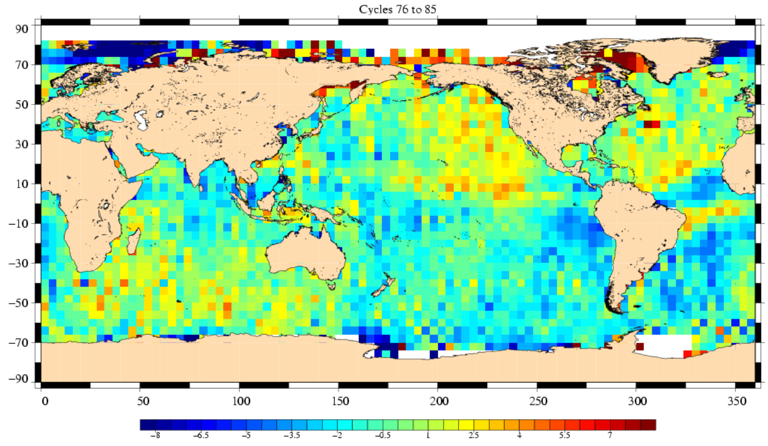

Figure 12: *Mean of SSH crossovers with old (top) and new (bottom) corrections in SSH*

An estimation has been computed with EIGEN-GRACE orbit and the old corrections to SSH (figure 13) and is compared to the previous estimate (figure 14). The values are close to each other in the regions of weak sea state conditions. For higher sea state conditions, a gradient appear progressively and can reach 3 cm for higher SWH and U values. This region is also impacted by the use of th MOG2D correction for Envisat, Jason and Topex altimeters as described in Labroue et al., [15]. Note also that a strong gradient appear above 6m and is representative of the lack of points in this regions.

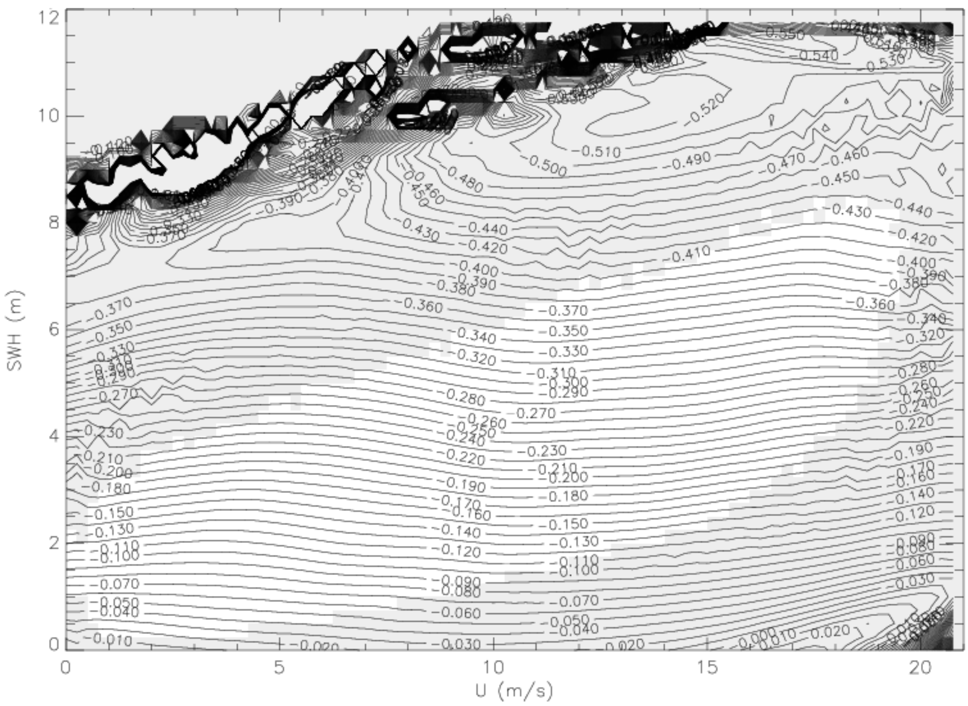

Figure 13: *SSB estimation using EIGEN-GRACE orbit and old corrections in SSH*

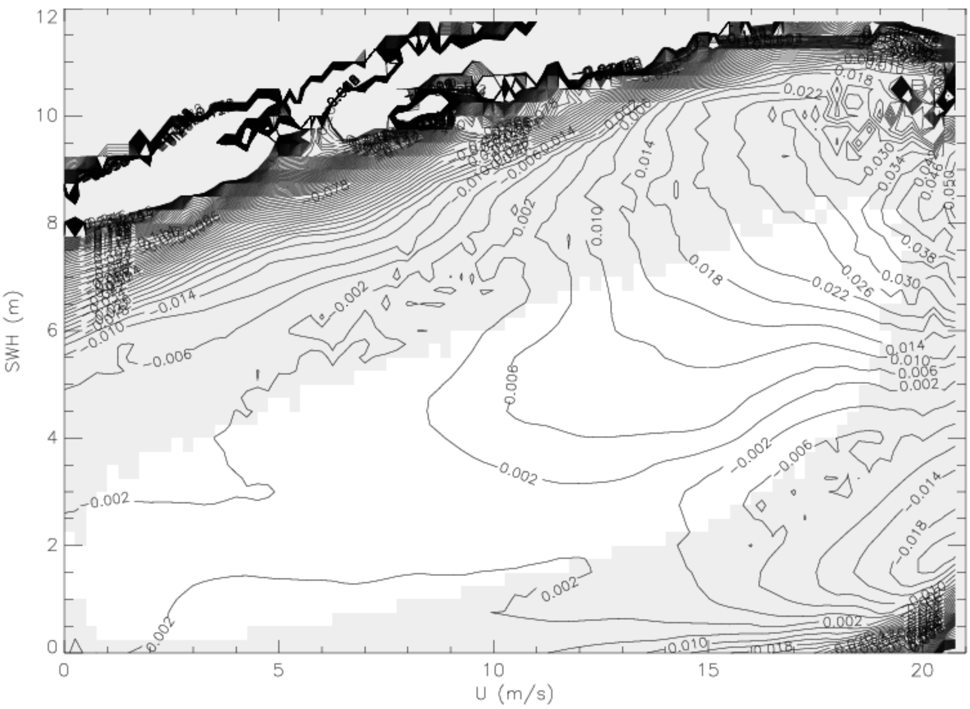

Figure 14: *Difference of SSB computed with EIGEN-GRACE orbit and new and old corrections in SSH*

3.5 Impact of orbits

The data set has been updated with the EIGEN-GRACE orbit delivered by Delft [4]. Figure 15 shows the SSH crossover differences using EIGEN-GRACE and DGME-04 (Scharroo and Visser, 1998 [20]) orbits. A preliminary estimation of the datation bias has been performed as explained in section 3.3. There is a strong hemispheric signal present in the DGME-04 orbit mainly in Pacific and Indian Ocean and still present with the Delft orbit but in a lesser extent.
The resulting SSB estimation is presented in figure 16. The difference with the previous estimate made with EIGEN-GRACE (figure 17) exhibits significant SWH gradients up to 3 cm for waves below 4m. Note that one part of the resulting difference maybe explained by the datation bias: indeed, Labroue et al., 2002 [14] showed that a value of 150 mcirosecond could lead to a gradient of 1 cm below 3m waves.

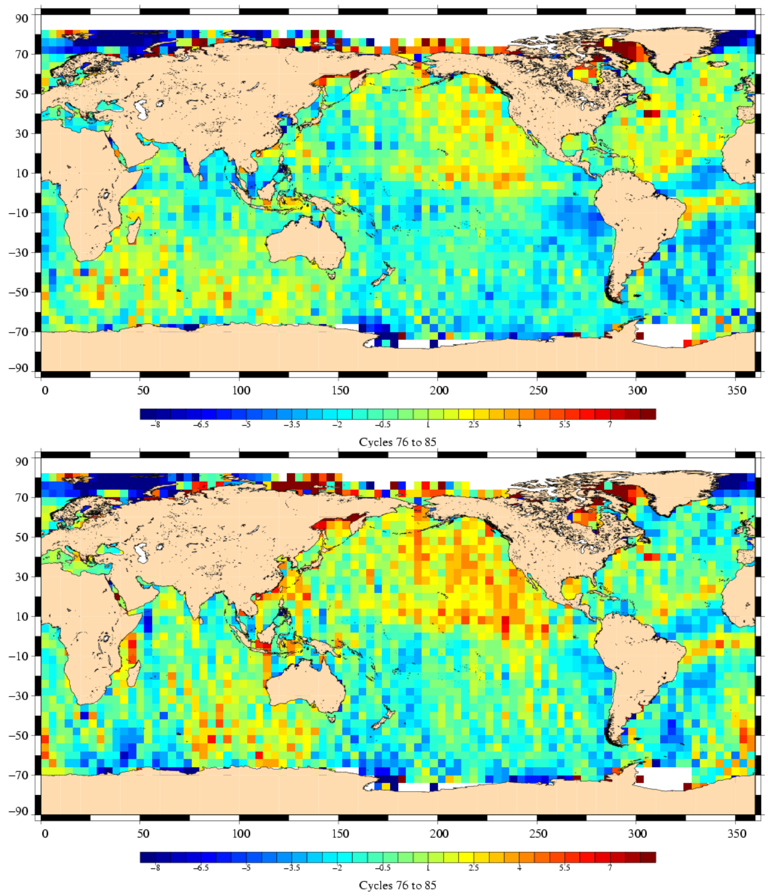

Figure 15: *Mean of SSH crossovers with EIGEN-GRACE (top) and DGME-04 (bottom) orbits with new SSH*

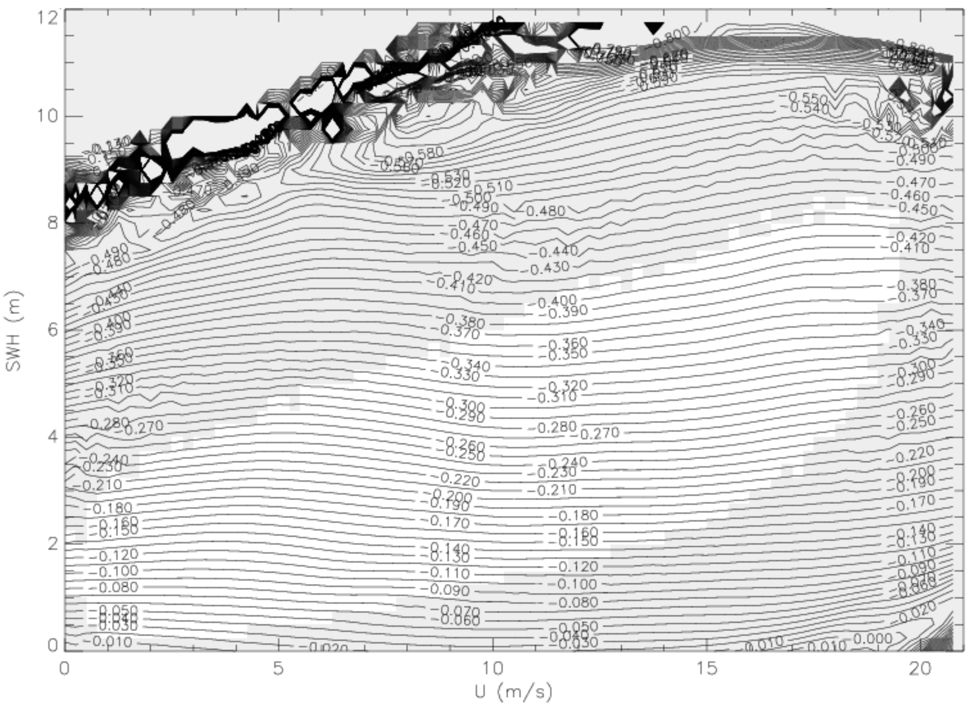

Figure 16: *SSB estimation using DGME-04 orbit and new corrections in SSH*

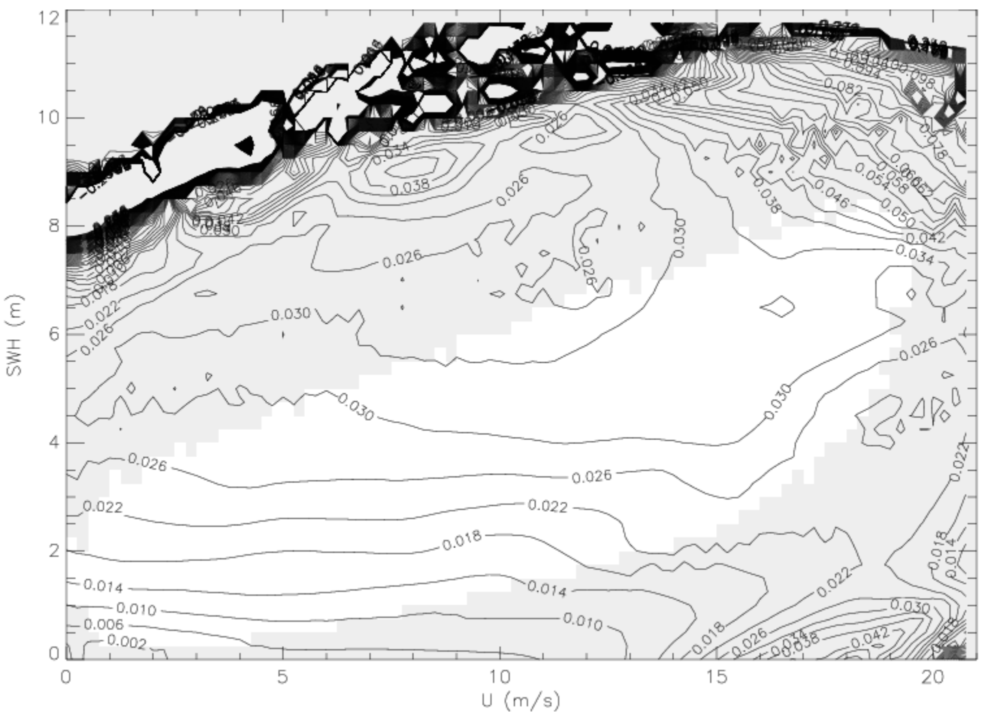

Figure 17: *Difference of SSB computed with EIGEN-GRACE and DGME-04 orbits*

3.6 Correction of orbit error

An orbit error is computed on each cycle by fitting a 1 and 2-cycle per revolution sinusoidal model. This allows removing the long wavelength errors. The impact on SSH differences at crossovers is shown in figure 18. Even if GIM ionosphere correction is used, there is still a signal visible at the equator in the Atlantic Ocean, which can be due to ionosphere correction still impacted by high solar activity.
The estimation made with a correction of orbit error (figure 19, compared to figure 11) shows less dependant behavior of SSB with wind speed, especially for low SWH values. The difference (figure 20) between the two exhibits some dependency with SWH when the sea state becomes stronger: (3m,10m/s). The gradient found for weak SWH may be less confident. Because there is still a marked hemispheric signal in the crossover differences, it is better to compute the SSB estimate with the fitting orbit error applied.

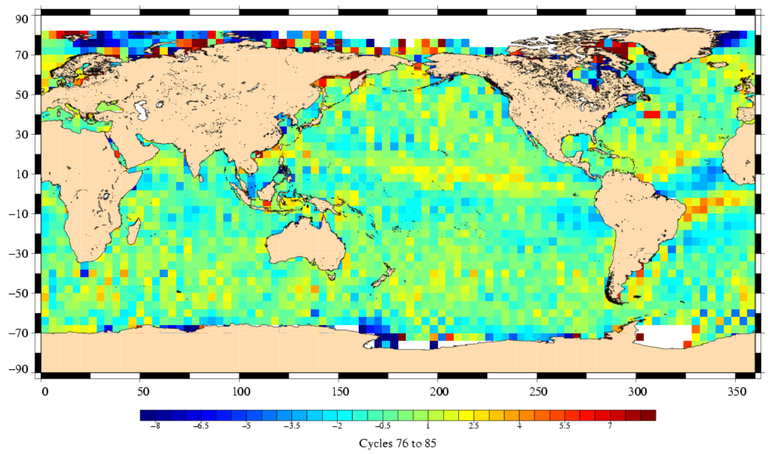

Figure 18: *Mean of SSH crossovers with EIGEN-GRACE orbit corrected for orbit error*

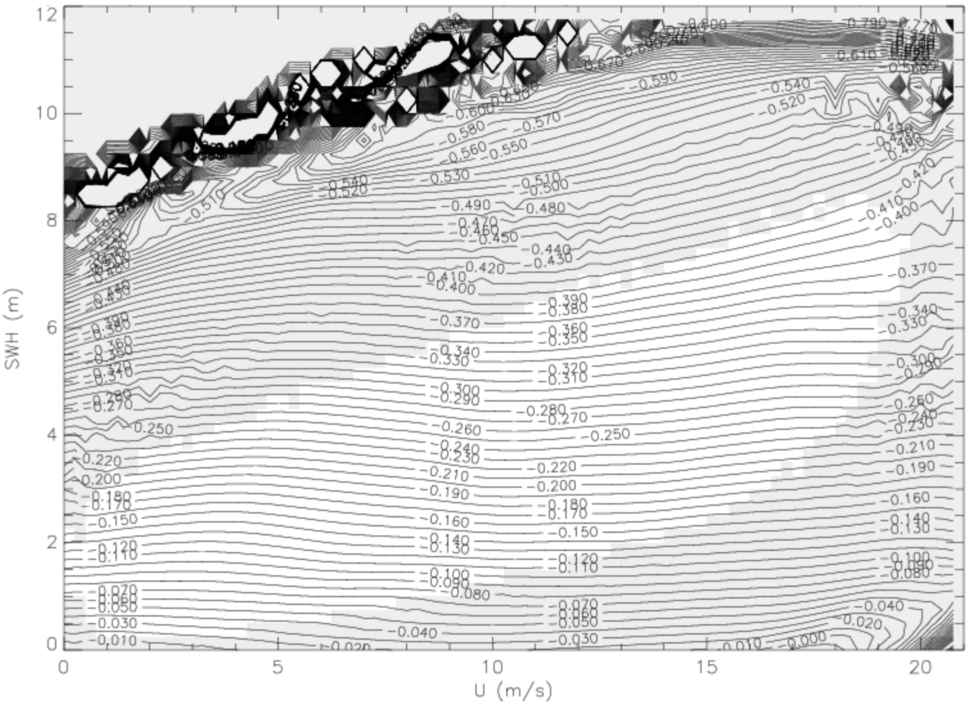

Figure 19: *SSB estimation using EIGEN-GRACE orbit corrected for orbit error*

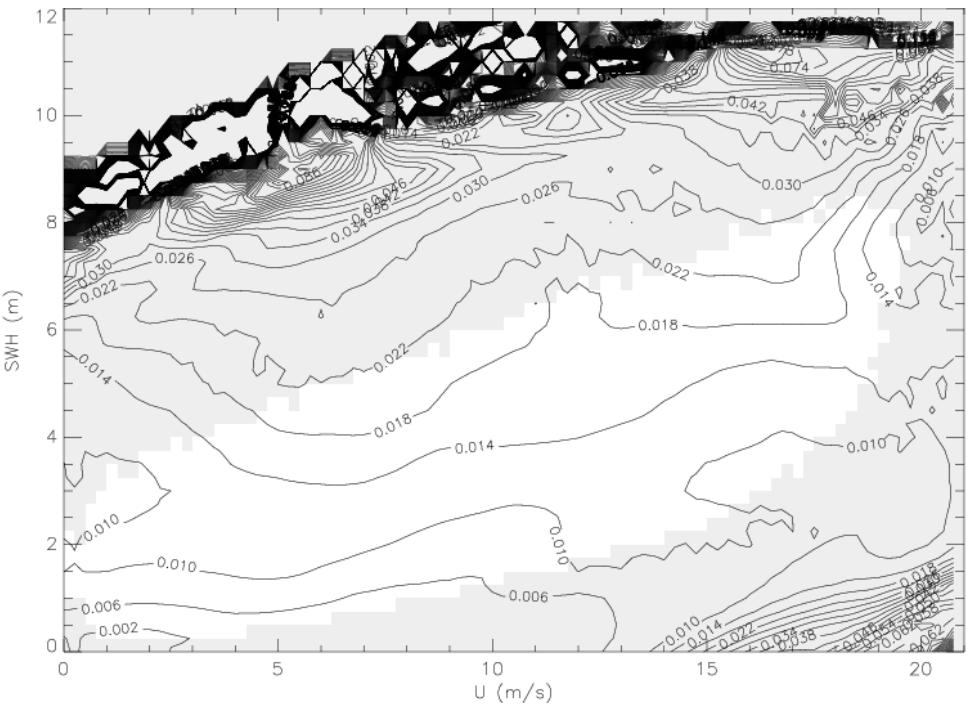

Figure 20: *Difference of SSB using EIGEN-GRACE orbit with and without orbit error*

3.7 Extended estimation over the whole definition set

The method described in Labroue et al., 2005 [15], has been applied to the final estimation (figure 21). It consists in computing a new smoothing factor in the regions where there are few or no data to extend the estimates of higher density areas. This technique enables to extend the SSB values in all the (U SWH) grid. The resulting SSB takes the same values as before in the areas where data are present and extend the shape of the function otherwise.

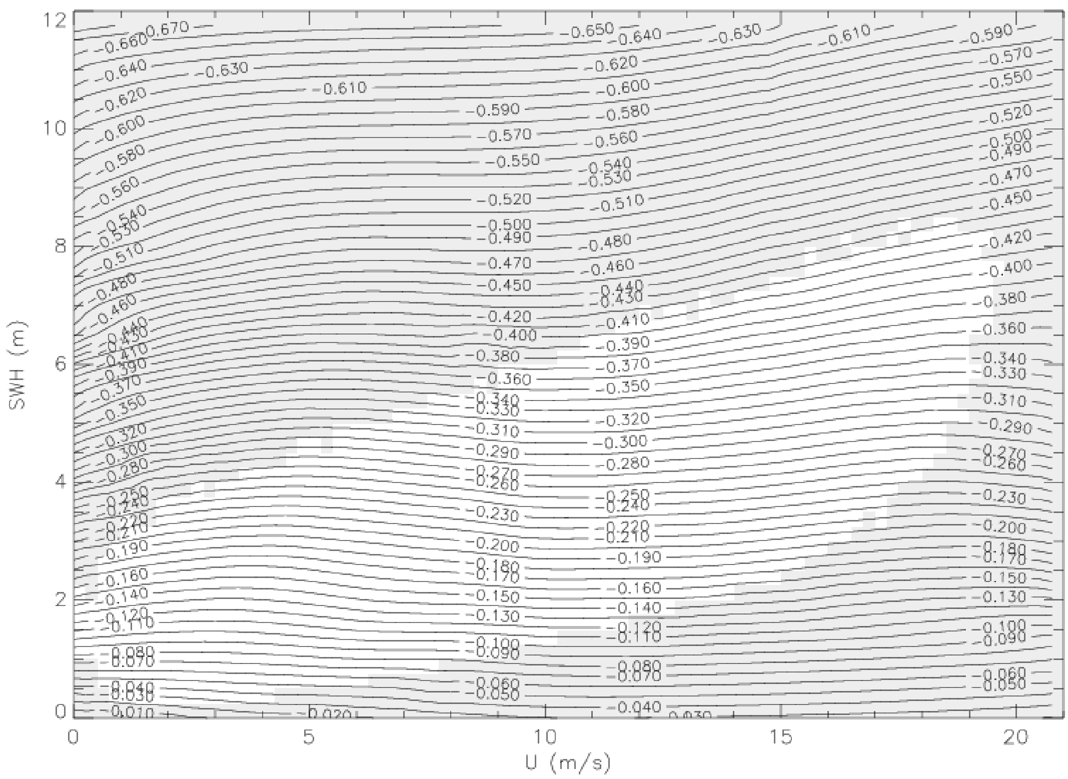

Figure 21: *SSB estimation with the new smoothing factor*

3.8 Estimations with Direct and Collinear methods

Given the results obtained with the method of crossovers, the SSB has also been computed with the direct and collinear method and are shown in figures 22 and 23 for the direct method and 24 and 25 for the collinear method. For the two estimations, the points with a bathymetry lower than 1000m and latitude below 66° are selected. The SSH used is the one from table 3, taking into account the "new" set of corrections. Moreover, the datation bias and the orbit error are included.
For the residuals, a same filtering as in crossovers is applied on the along-track computation of the SSH and SWH : 6cm and 40cm noise in the spline fitting.
The direct method exibits an unexpected behaviour in the region of strong sea state conditions. The comparison to the crossover shows also some high gradients for low wind speed, which is not the case for the comparison to collinear method and shows the impact of filtering for such (SWH,U) values. The difference between collinear and crossover methods shows surprisingly some SWH gradients. One reason for that difference should be explained by the use of the ionosphere model correction, with a weak impact on the residuals since the orbit is sun-synchronous. Another explanation comes from the use of the orbit error correction, which is computed as a minimisation of crossovers.

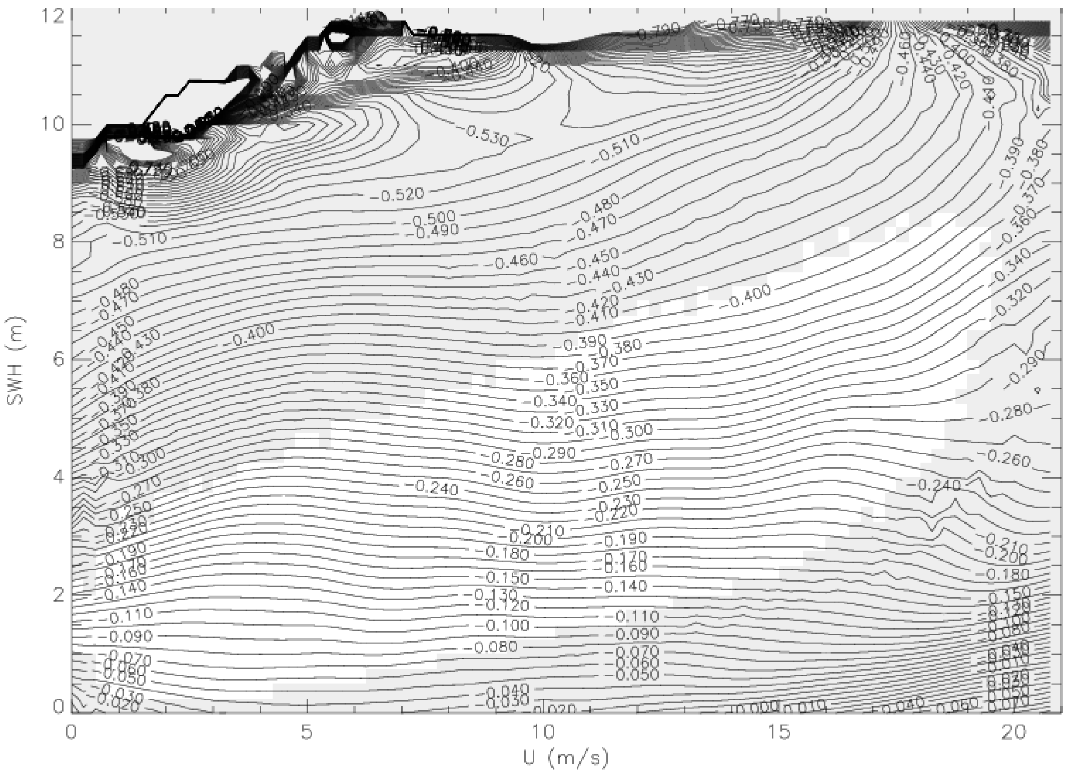

Figure 22: *SSB estimate obtained with direct method*

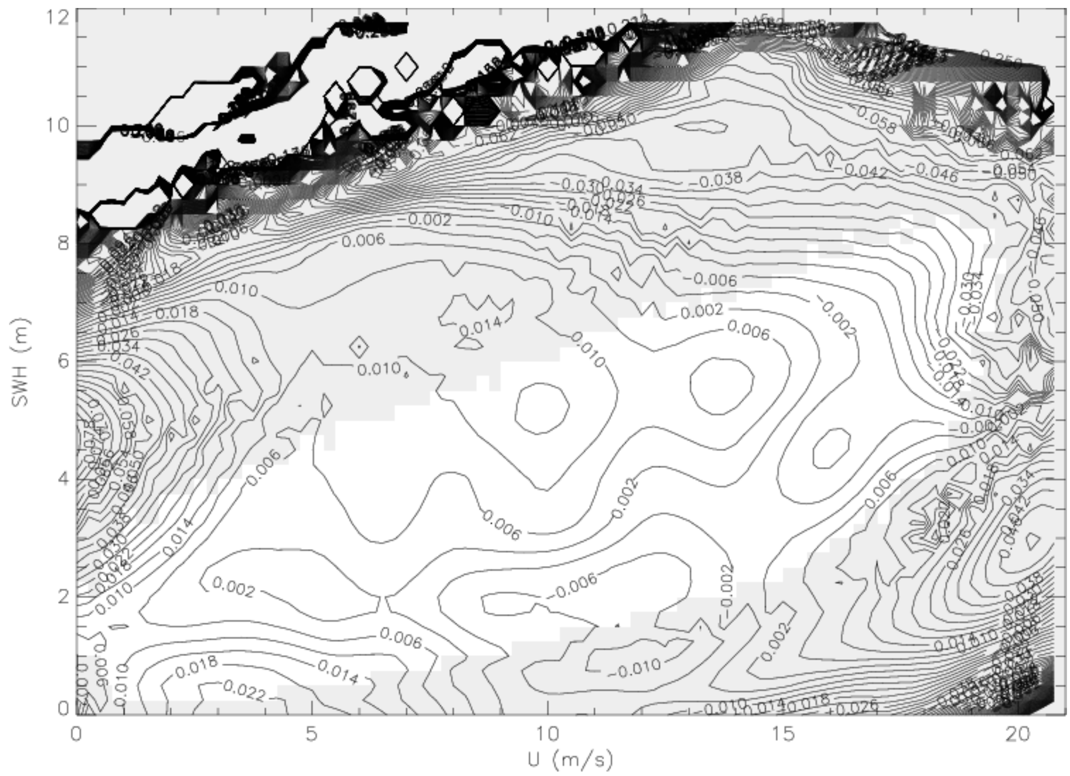

Figure 23: *Difference SSB from direct and crossover methods*

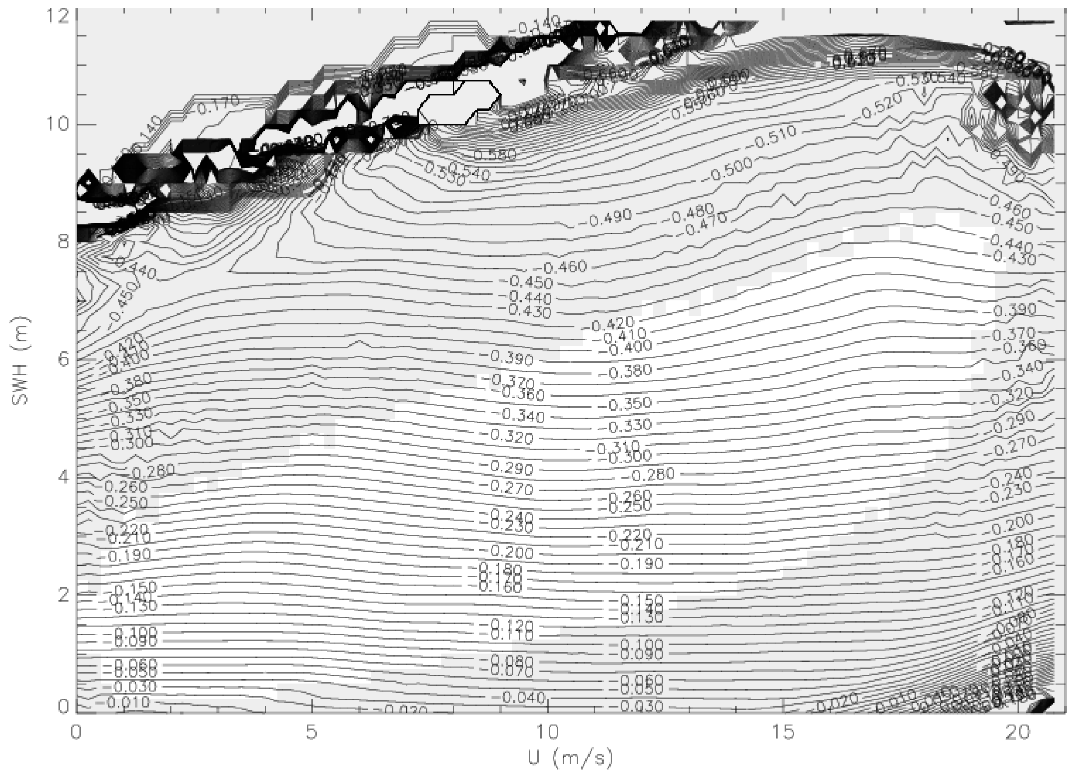

Figure 24: *SSB estimate obtained with collinear method*

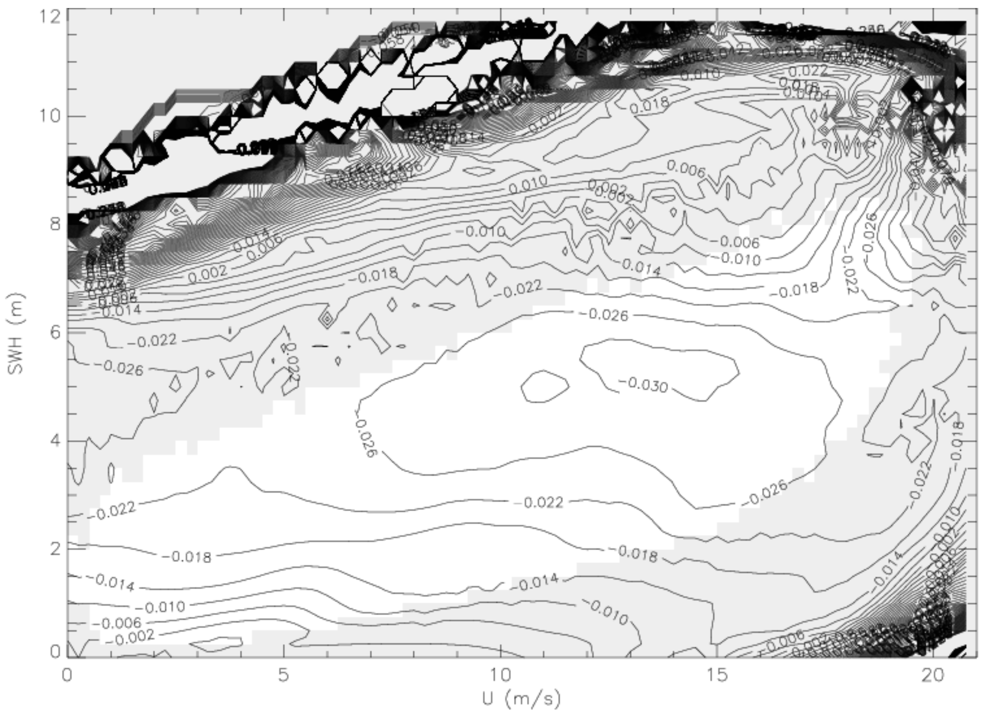

Figure 25: *difference SSB collinear and crossover methods*

3.9 Statistical results

On the basis of 10 cycles, statistical results have been obtained by comparing the SSH with BM3 model against the other 3 methods. The results are very close from one model to each other (see in table 4). The gain in variance for the crossover estimation is respectiveley 0.68 cm^2 and 0.73 cm^2 along-track and at crossovers. Surprisingly, the collinear estimation gives good results at crossovers. The most significative features appearing on maps of differences of variance comes from the crossover method as shown on figures 26 and 27. The negative values indicate a gain in variance of the new correction compared to BM3 model. The most impact is visible in the Indian Ocean and Indonesia. Some improvement is aslo noticeable in tropical Atlantic where there is a strong ionospheric signal.

SSH formula	along-track	at crossovers
with BM3 estimation	11.36	9.20
with crossover estimation	11.33	9.16
with collinear estimation	11.36	9.15
with direct estimation	11.32	9.18

Table 4: *Standard deviation (cm) of SSH at crossovers and along-track using several configurations*

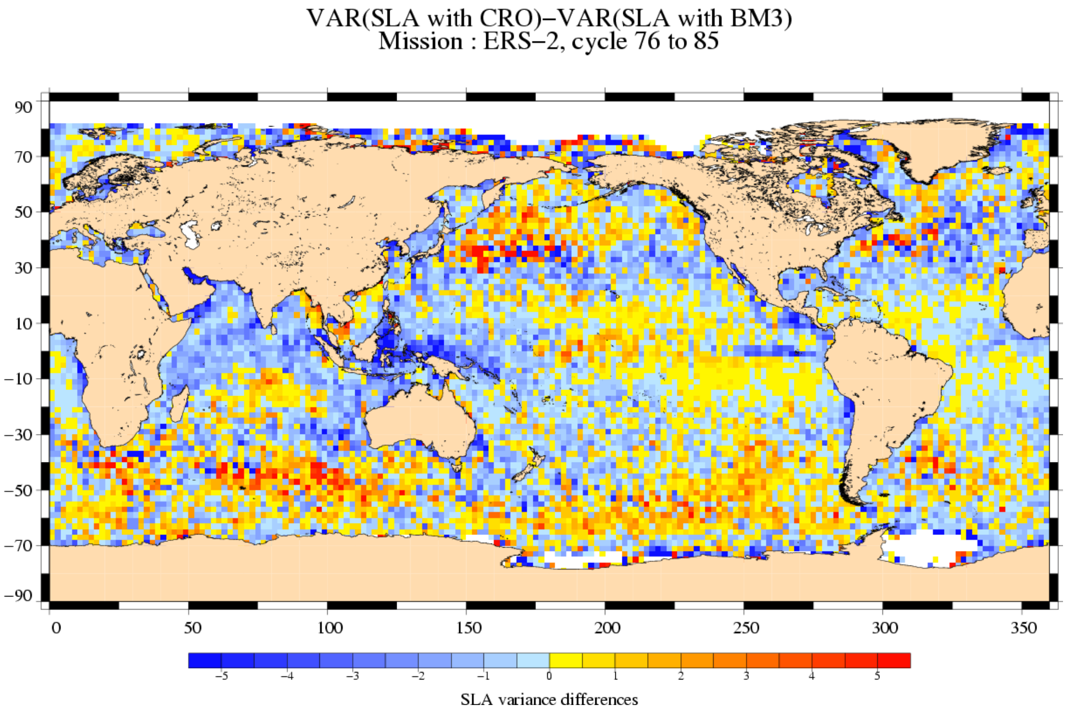

Figure 26: *difference of variance (cm^2) along-track*

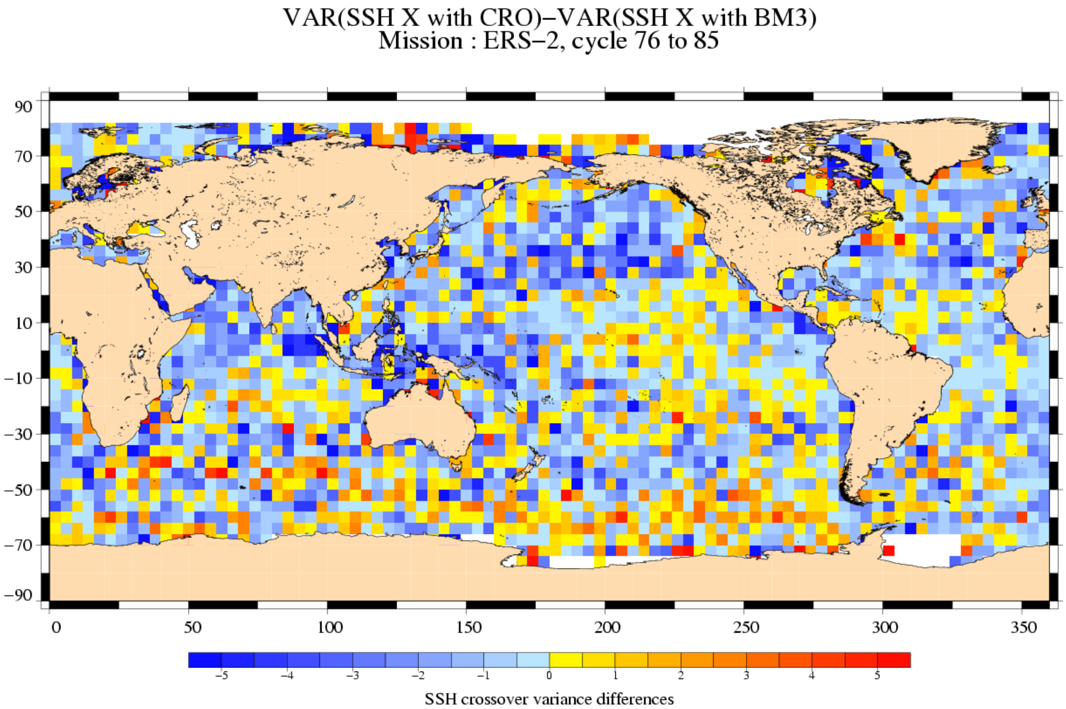

Figure 27: *difference of variance (cm^2) at crossovers*

3.10 Comparison to Envisat SSB

The difference to Envisat SSB estimate (figure 28) from Labroue, 2005 [15] exhibits some SWH gradients from 1 cm for low SWH and up to 10 cm for strong sea state conditions, which represent roughly a difference of 1.5% in SWH as expected.

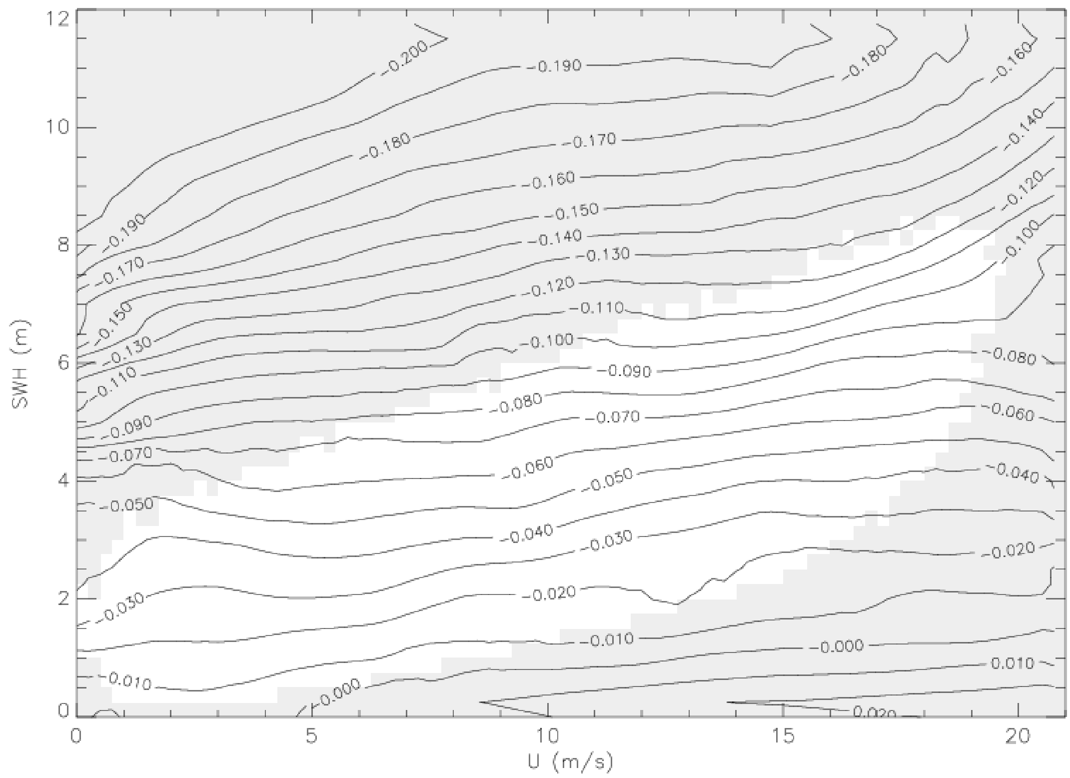

Figure 28: *Difference of (Envisat - ERS-2) SSB estimates*

3.11 Conclusion

The SSB estimate is now computed from filtered SSH and SWH crossovers and with a larger smooth window parameter. Once those parameters have been fixed, it was possible to estimate a SSB using the new algorithms provided for Envisat and Jason altimeters. Such corrections are significant in terms of SSB correction and the consistency with other altimeters has been evidenced. The impact of the new EIGEN-GRACE orbit has been assessed with a preliminary correction of adapted datation bias and it is still usefull to correct for the orbit error to have as best as possible input data to perform the estimation. The direct and collinear method have also been performed with the new set of corrections and statistical comparisons showed a very good consistency between the three methods. Nevertheless, the crossover method appear to be the best estimation in terms of minimizing the variance, even though the collinear method gives surprisingly good results for the global statistics. Nevertheless, some work is still needed to understand the behavior of such an estimation, notably because the orbit is sun-synchronous.

4 Improvement of the treatment of ERS-2 over coastal areas

4.1 Introduction

Coastal areas represent a unique but complex environment at the convergence point of atmospheric, oceanic and continental masses. Among numerous other specificities, these areas host the largest concentration of living resources and people on the planet. It is necessary to improve our knowledge of the functioning of the ocean at its limits.
Satellite altimetry has been originally conceived and successfully applied to study and monitor the open ocean. Data acquired in the immediate vicinity of emerged lands are often neglected because of their lower quality. Now that satellite altimetry is mature over open oceans, a challenging purpose consists in being able to accurately measure the sea level fluctuations near the coasts.

4.2 Context of the study

Hereinafter, coastal areas are defined as the zones located in the range 0-50 km from the shoreline, without any consideration of the bathymetry. Due to its large footprint, it is usually considered that radiometer measurements are polluted by emerged land up to 50 km away from the shoreline. For the altimeter, which footprint is much smaller, exploitable measurements can be acquired nearly up to the coast since satellite altimetry is used over rivers smaller than 1 km width. In fact, it is often the lack of a reliable radiometric correction that restricts the use of the corresponding (but existing !) altimetric measurements. Note however that other corrections (notably the ocean tide) often default near the coasts.
The first step of the present study consists in geographic and geometric calculations aiming at precisely computing the distance between each altimetric measurement and the closest shoreline point. The goal of the second step is to associate a realistic wet tropospheric correction to each altimetric measurement whose radiometer correction defaults. In the third step, we review the editing process by differencing the selection criteria over the open ocean and the coastal zones and try to recover a larger number of points over coastal areas. The final step is the computation of a global mean profile that takes advantage of the above developments above coastal areas.

4.3 1st step: precise computation of the distance between the altimetric measurement and the shoreline

In the ERS-2 products, the vicinity of the coasts is indicated by 2 flags: one for the altimeter and one for the radiometer. These flags are computed from land/sea grid masks which resolution (10'x10') is not always compatible with the possibly complex shape of the shoreline. Based on a previous internal study performed at CLS for Topex/Poseidon data, the ERS-2 theoretical tracks used at CLS have been recomputed with the inclusion of the following parameters for each 1-Hz position:

- new precise land sea mask,
- smallest distance to the shoreline,
- longitude and latitude of the closest land point,
- smallest distance to the shoreline along-track,
- longitude and latitude of the closest land point along track.

These parameters are computed using the geographical database of the GMT software (Wessel and Smith, 1999, [9]), from which local high-resolution land/sea masks (0.01° x 0.01°) are created near emerged lands. Each pass of each cycle has then been projected over these theoretical tracks to compute the above parameters for each given altimetric measurement. In the following example, we reproduce these parameters (table 5) for track 702, cycle 40, near Sicily and we visualize and check these data with a GIS software (figure 29).

Longitude (degrees)	Latitude (degrees)	mask	ShoreLon (degrees)	ShoreLat (degrees)	Dist (km)	ShoreLon (degrees)	ShoreLat (degrees)	Dist (km)
			Along Track			Across Track		
14.769962	38.615212	0	14.577796	38.059661	64.268	14.805	38.575	6.663
14.751676	38.557635	0	14.577796	38.059661	57.663	14.805	38.565	5.987
14.733412	**38.500057**	**0**	**14.577796**	**38.059661**	**51.058**	**14.805**	**38.555**	**9.4**
14.715171	38.442478	0	14.577796	38.059661	44.454	14.805	38.555	15.086
14.696957	38.384910	0	14.577796	38.059661	37.850	14.585	38.555	20.235
14.678761	38.327326	0	14.577796	38.059661	31.246	14.745	38.165	19.924
14.660587	38.269739	0	14.577796	38.059661	24.640	14.745	38.165	14.989
14.642434	38.212150	0	14.577796	38.059661	18.035	14.735	38.155	11.687
14.624309	38.154573	0	14.577796	38.059661	11.431	14.685	38.105	8.982
14.606202	38.096979	0	14.577796	38.059661	4.826	14.605	38.065	4.271
14.588116	38.039383	1	14.577796	38.059661	-1.779	14.575	38.065	-2.336

Table 5: *Values of Shoreline parameters for pass 702 in cycle 40*

We check that for the point at latitude 38.500057 (green star) we measure 51.1 km and 9.3 km for the along-track and across-track shoreline distances respectively, whereas our computation gives 51.058 km and 9.4 km respectively (see table 5). The computed corresponding closest points along track and across-track, symbolized by the blue and yellow stars respectively appear fully realistic. The most important parameter resulting from this first step is the across-track distance to the coast. It will be widely used in the following step. Note also that this parameter can be used to defined new precise altimeter/radiometer land flags if necessary.

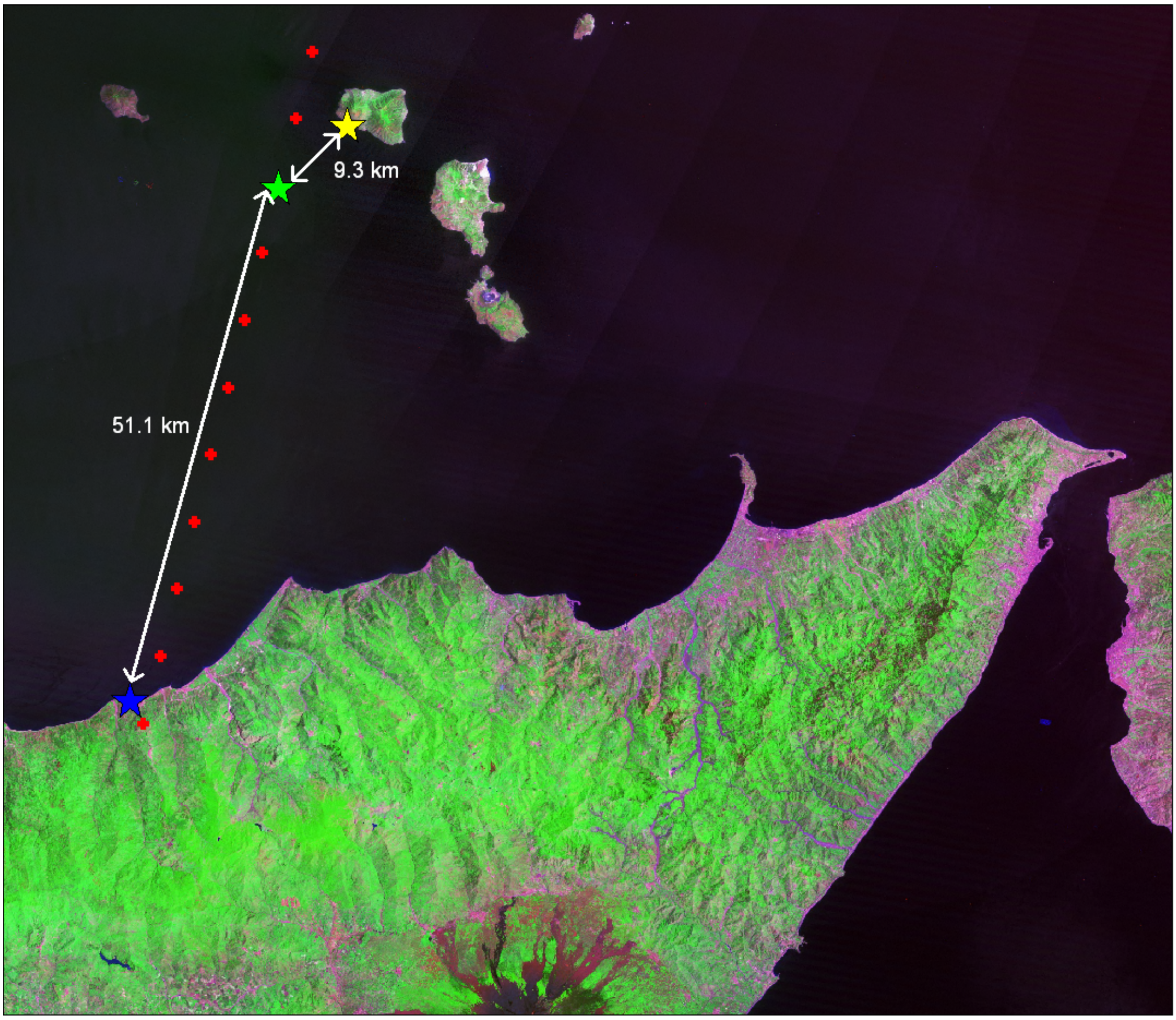

Figure 29: *Example for pass 702*

4.4 2nd Step: computing a realistic wet tropospheric correction where the radiometer defaults

4.4.1 Introduction

When the radiometer correction is missing or should not be used (erroneous values and/or vicinity of the coasts and ice), it is fundamental to be able to replace it by a realistic wet tropospheric correction. Without such a strategy, lots of valuable altimeter measurements that do not have a corresponding radiometer correction have to be rejected in the usual data processing, especially near the coasts. Basic approaches have already been used:

- simple use of the model correction: it may introduce steps in the corrected signal,
- interpolation of the radiometer correction over "small holes" ($<$ 32 s, i.e. 200 km),
- replication of the last valid radiometer correction in the edges of the tracks: plateau in the correction profile.

The principle and the objectives of our method are to combine and enhance the above approaches by identifying a set of configurations receiving dedicated correcting strategies.

4.4.2 Definition of the different configurations and correcting strategies

Given a series of configurations hearafter described, the computation of the new wet troposphere correction (noted composite correction: CompositeWetTropoCorr is performed. The first two obvious configurations of points to take into account are:

- the Continental Mass (hereafter denoted Continental_Mass) where the bathymetry is positive and correspond to several consecutive measurements with a hole of more than 32 seconds. For those measurements, no wet troposphere correction has to be computed.
- the points with the radiometer wet troposphere correction valid (i.e. between 0 and 50 cm) hereafter denoted Radiometer_OK.

Two categories of measurements with the distance to Shoreline < 50 km and a negative bathymetry are identified:

- the coastal path (Coastal_Path) where the track segment is encontoured at each end by the Continental_Mass configuration. The model correction is taken :
  CompositeWetTropoCorr = WetModTropoCorr
- the transition mode with a Continental_Mass configuration at one end of the track segment and Radiometer_OK at the other end. The new correction is computed as follows:

  1. Computation of DeltaCorr at the last point of the segment where WetRadCorr is valid:
     DeltaCorr = WetModCorrLast - WetRadCorrLast
  2. and then CompositeWetTropoCorr = WetModTropoCorr - DeltaCorr

  Note that this strategy takes advantage of the dynamics of the model and does not introduce any step in the correction profile.

The two other possible configurations (independant of the distance to shoreline) are:

- the small hole (Small_Hole) which has a duration < 32 s in the radiometer correction profile with Radiometer_OK correction at both ends of the hole.

Then the correction is computed if bathymetry < 0, and is a linear interpolation based on the valid radiometer corrections of each end of the segment. Note that the hole can be due to missing/erroneous radiometer values over the open ocean as well as to the presence of emerged land below or near the tracks.

- the big hole (Big_Hole) which has a duration > 32 s in the radiometer correction profile with Radiometer_OK correction at both ends of the hole. The new correction is computed as follows:

  1. Computation of DeltaCorrBefore and DeltaCorrAfter at each end of the hole:
     DeltaCorrBefore = WetModCorrBefore- WetRadCorrBefore
     DeltaCorrAfter = WetModCorrAfter - WetRadCorrAfter
  2. Computation of DeltaCorr as the mean:
     DeltaCorr= (DeltaCorrAfter + DeltaCorrBefore) /2
  3. and computation of the new correction:
     CompositeWetTropoCorr = WetModCorr - DeltaCorr.
  4. Then smoothing of the new correction at the edges of the segment: the direct application of the above algorithm does not prevent from possible steps at the edges of the corrected signal. Therefore, we smooth these potential steps by applying, at each end of the segment, a linear interpolation between the last valid radiometer correction and the 6^{th} newly computed correction (towards the centre of the hole).

  Note that the hole can be due to missing/erroneous radiometer values over the open ocean as well as to the presence of emerged land (that are not a Continental_Mass) below or near the tracks.

The last possible configuration:

- Track_end with negative bathymetry where there are no valid radiometer measurement between the end of the track and a Continental_Mass configuration. The correction proposed is the model.

4.4.3 Examples

Figure 30 is a map example of these various configurations over the Mediterranean Sea for cycle 040.

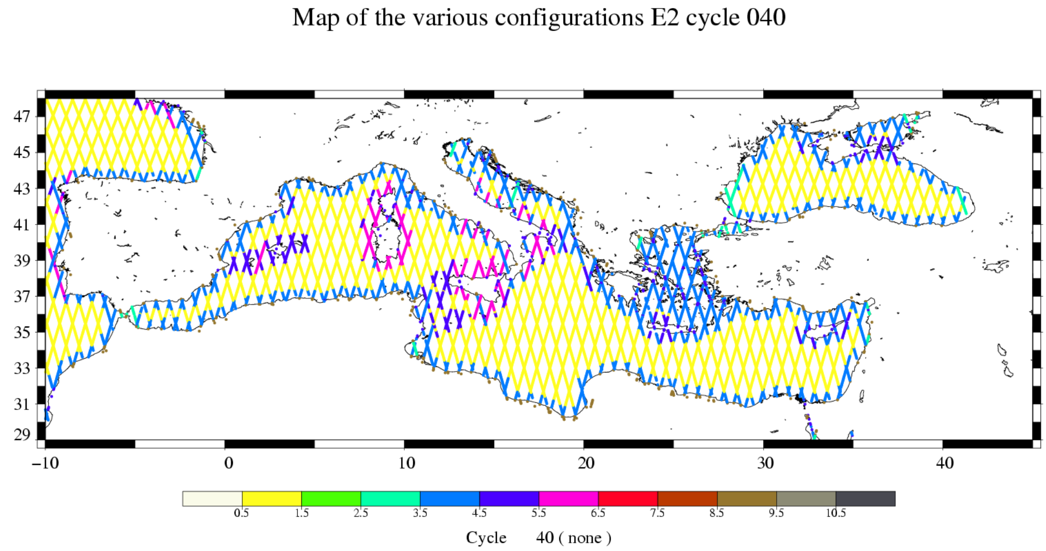

Figure 30: *Configurations in Mediterranean Sea: 1=Radiometer_OK, 3=Coastal_Path, 4=Transition, 5=Small_Hole, 6=Big_Hole, 9=Continental_Mass, 10=Track_End*

In figure 31, we reproduced the fluctuations of the radiometer, model and "new" composite wet tropospheric corrections for track 702 over the Mediterranean Sea. At first, this track crosses the Adriatic Sea between 42°N and 43.5°N. There are always emerged lands closer than 50 km (42 km at maximum): the composite correction is the model correction. Then, ERS-2 flies over Italy, with a transition zone (the model correction is shifted to the level of the closest valid radiometer correction), followed by a few points acquired in open ocean conditions (we keep the radiometer correction). After that, the ERS-2 arrives over Sicily, that is considered as a "Big Hole" and continues in open ocean conditions up to the African coast (transition). On that figure, we clearly see that the radiometer correction exhibits large and spurious fluctuations in the vicinity of emerged land, whereas the new composite correction profile appears more realistic, taking advantage of the valid radiometer correction values and of the model dynamics.

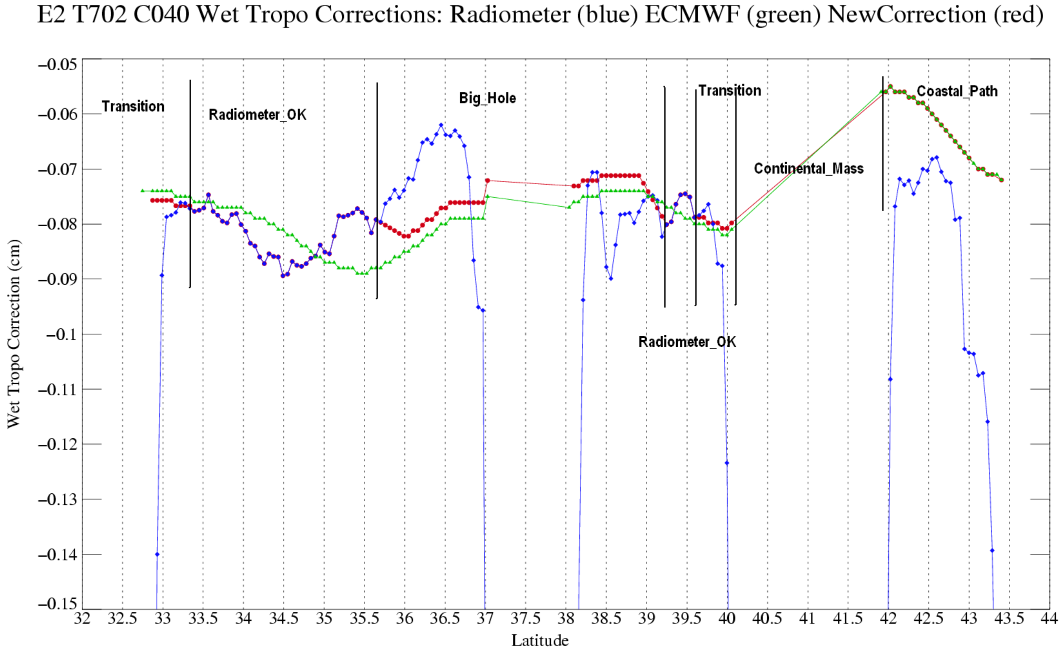

Figure 31: *Radiometer, model and composite wet troposphere correction profiles for pass 702, cycle 040*

4.4.4 Conclusion

As a conclusion for that part, we can state that the various configurations identified above allow us to propose a correction strategy customized for each configuration. Consequently, we are able to associate a realistic wet tropospheric correction to each valid altimetric measurement, regardless of its distance to the coasts.

4.5 3rd Step: Data Editing

4.5.1 Introduction

The data editing process is necessary to remove altimeter measurements having lower accuracy. Detailed description of this process is given is QA reports (Mertz et al., 2005 [18]).

4.5.2 Usual editing parameterization

The regular editing criteria are summarized in the table below, with an example of results for cycle 40.

	Open ocean			**Coastal areas**		
Total number of measurement	1677819			142796		
Step 1: Flags	Number / percentage of points removed			Number / percentage of points removed		
Manoeuvre flag	2261 / 0.13			87 / 0.06		
Ice Flag	87918 / 5.24			44718 / 31.32		
Results: initial, rejected, final	1677819 / 100.0	90029 / 5.37	1587790 / 94.63	142796 / 100.0	44750 / 31.34	98046 / 68.66
Step 2: Parameters	Lower boundary	Upper boundary	Number / percentage of points removed	Lower boundary	Upper boundary	Number / percentage of points removed
Sea Surface Height from product (m)	-130	100	48 / 0.00	-130	100	720 / 0.50
Number of 20 Hz measurements	10	-	403 / 0.02	10	-	7296 / 5.11
Std Deviation of 20 Hz measurements (m)	0.0	0.450	11464 / 0.68	0.0	0.45	10809 / 7.57
Smoothed off-nadir angle (deg) *	-0.16	0.16	0 / 0.00	-0.16	0.16	0 / 0.00
Dry tropospheric correction (m)	-2.5	-1.9	0 / 0.00	-2.5	-1.9	0 / 0.00
Radiometer wet tropospheric correction (m)	-0.5	0.0	107 / 0.01	-0.5	0.0	912 / 0.64
Atmospheric forcing (MOG2D) (m)	-2.0	2.0	0 / 0.00	-2.0	2.0	0 / 0.00
Ionospheric correction (m)	-0.2	-0.001	0 / 0.00	-0.2	-0.001	0 / 0.00
Significant wave height (m)	0.0	10.0	1668 / 0.10	0.0	10.0	1973 / 1.38
Electromagnetic Bias (BM3)	-0.7	0.0	1623 / 0.10	-0.7	0.0	1991 / 1.39
Sigma naught (dB)	6.0	30.0	1722 / 0.10	6.0	30.0	1224 / 0.86
Ocean tide height (FES04) (m)	-5.0	5.0	4 / 0.00	-5.0	5.0	3145 / 2.20
Solid earth tide (m)	-1.0	1.0	0 / 0.00	-1.0	1.0	0 / 0.00
SSH from product – CLS01V1 MSS (m)	-2.0	2.0	3107 / 0.19	-2.0	2.0	7726 / 5.41
Results: initial, rejected final	1587790 / 94.63	13579 / 0.81	1574211 / 93.82	98046 / 68.66	13648 / 9.56	84098 / 58.89

Table 6: *Usual parameterization of the Editing process*

A final editing is performed on corrected sea surface height for the whole oceanic domain (open ocean + coastal areas), using a spline fitting procedure, leading to remove 1576 / 0.09 % additional points. At the end of the process, 163882 points (9.00 %) are rejected, leaving 1656733 points (91.00 %) valid. During step 2, most of the points are rejected by the "std deviation of 20 Hz measurements" criteria. For coastal areas, data points are expected to be gained also for the following criteria:

- SSH minus MSS,
- Number of 20 Hz measurements,
- Ocean tide height.

4.5.3 New parameterization for coastal enhancement

Most of the measurements rejected by the usual editing process are located near the coasts. It is not surprising: the above criteria are optimized for the open ocean where the measurement conditions are optimal and are therefore supposed to be too restrictive for the coastal areas where the measurement conditions are degraded. Too few data are selected near the coasts where, for example, it is difficult to compute reliable mean profiles. The objective of the present study is to find an acceptable compromise between the quality of the data, (that is necessarily lower over coastal areas) and the number of selected measurement (that needs to be increased).

We thus defined a dual editing parameterization that:

- keeps almost unchanged the usual criteria over the open ocean,
- introduce less restrictive criteria over coastal areas (distance to shoreline < 50 km).

However, supplementary tests have been added for both domains:

- Step 1: the test on the Land/sea mask which computation is described above and a test on bathymetry,
- Step 2: the radiometer correction is replaced by the new composite wet tropospheric correction described above. For the coastal areas, we modified the lower/upper boundaries for the number and standard deviation of 20 Hz measurements, as well as for the smoothed off-nadir angle, just because these tests reject most of the points. Finally, since the MSS is not as accurate over coastal areas as over the open ocean, we did not apply the test based on the difference between SSH and MSS.

These criteria are gathered in the table 7:

	Open ocean			Coastal areas		
Total number of measurement	1677819			142796		
Step 1: Flags	Number / percentage of points removed			Number / percentage of points removed		
Manoeuvre flag	2261 / 0.13			87 / 0.06		
Ice Flag	87918 / 5.24			44718 / 31.32		
Land/Sea Mask = 0	0 / 0			20228 / 14.17		
Bathymetry <0	472 / 0.03			22669 / 15.88		
Results : initial, rejected, final	1677819 / 100	90326 / 5.38	1587493 / 94.62	142796	53118 / 37.20	89680 / 62.80
Step 2: Parameters	Lower boundary	Upper boundary	Number / percentage of points removed	Lower boundary	Upper boundary	Number / percentage of points removed
Sea Surface Height from product (m)	-130	100	48 / 0.00	-130	100	68 / 0.05
Number of 20 Hz measurements	10	-	399 / 0.02	3	-	625 / 0.44
Std Deviation of 20 Hz measurements (m)	0.0	0.450	11427 / 0.68	0.0	1.35	1661 / 1.16
Smoothed off-nadir angle (deg) *	-0.16	0.16	0 / 0.00	-0.36	0.36	0 / 0.00
Dry tropospheric correction (m)	-2.5	-1.9	0 / 0.00	-2.5	-1.9	0 / 0.00
New wet tropospheric correction (m)	-0.5	0.0	9 / 0.00	-0.5	0.0	316 / 0.22
Atmospheric forcing (MOG2D) (m)	-2.0	2.0	0 / 0.00	-2.0	2.0	0 / 0.00
Ionospheric correction (m)	-0.2	-0.001	0 / 0.00	-0.2	-0.001	0 / 0.00
Significant wave height (m)	0.0	10.0	1666 / 0.10	0.0	10.0	565 / 0.40
Electromagnetic Bias (BM3)	-0.7	0.0	1621 / 0.10	-0.7	0.0	374 / 0.26
Sigma naught (dB)	6.0	30.0	1722 / 0.10	6.0	30.0	170 / 0.12
Ocean tide height (FES04) (m)	-5.0	5.0	4 / 0.00	-5.0	5.0	185 / 0.13
Solid earth tide (m)	-1.0	1.0	0 / 0.00	-1.0	1.0	0 / 0.00
SSH from product – CLS01V1 MSS (m)	-2.0	2.0	3094 / 0.18	-	-	0 / 0.00
Results : initial, rejected final	1587493 / 94.62	13489 / 0.80	1574004 / 93.81	89680 / 62.80	3083 / 2.16	86597 / 60.64

Table 7: *New paramaterization of the Editing process*

The same spline fitting procedure as described above is applied, leading to remove 3283 / 0.20 % additional points. At the end of the process, 163299 points (8.97 %) are rejected, leaving 1657316 points (91.03 %) valid.

4.5.4 Analysis of the results

The results of the Editing process are examined distinctly over 2 domains. In the Open Ocean, as expected, the difference between the 2 editing procedures is not significant (90 points, 0.01%). In Coastal areas, 8368 additional points are rejected in step 1 due to the introduction of the new tests based on the accurate localization of the measurement points. Results of step 2 suggest that most of these points, located over lands, were previously rejected during Step 2. For that reason, it has not been necessary to modify all the boundaries in Step 2. The number of points rejected by each parameter in step 2 is lowered to a level we consider acceptable. The most restrictive criterion is now the standard deviation of 20 Hz measurements. The new wet tropospheric correction rejects only 316 points versus 912 with the radiometer correction. At the end of step 2, we note an increase of 1.75 % of the number of valid points: about 2500 points are recovered. However, it appears that the spline fitting procedure rejects a large part of these points since the final number of valid points only increases by 583 (i.e. less that 1 point per track). Only 2.16 % points are rejected at the end of step 2: a further enlargement of the various boundaries would be useless.

4.5.5 Conclusion

As a conclusion, we found that the initial editing criteria over coastal areas are not as restrictive as previously thought. A significant number of data points were not properly rejected at the first step of the editing (quality flags) but were nevertheless rejected at the following step (parameter thresholds). With the proposed parameterization, land points are now identified (and rejected!) at the beginning of the process. We showed that finally, only a very limited number of points can be gained over coastal areas. Nota: for cycle 40, the smoothed off-nadir angle is not computed. The new boundaries for that parameter have been computed from a similar analysis performed on cycle 71.

4.6 4th Step: Computation of a new mean profile

4.6.1 Introduction

In the usual processing routinely performed at CLS, the mean profiles are mainly used to compute residuals from which Sea Level Anomalies are processed. The existing mean ERS profile used at CLS has been computed on the former VAX/VMS environment of CLS, with routines that have themselves evolved during the migration towards the actual Unix/Linux environment. This means that this profile could not be exactly reproduced. Moreover, this profile had been computed using ERS-1 and ERS-2 (63 cycles from October 1992 to December 1993 and from Mars 1995 to January 2000) data whereas for the present study, we only use ERS-2 data, from cycle 1 to cycle 85 (May 1995 to June 2003). Several internal studies realized at CLS spotted out spurious fluctuations of this profile near the coasts, where mean points are often computed with a limited number of measurements. Note however that this profile, at the contrary to the equivalent profile used at CLS for Topex/Poseidon, contains mean points that are very close to the shoreline. For all these reasons, it has been decided to reprocess it.

4.6.2 Objective

The objective of this part of the present study is twofold: increase the number of measurements used in the computation of each point of the mean profile, compute points as close as possible from the coast. For that purpose, the whole ERS-2 data base at CLS has been updated with the above developments, and the new mean profile has been computed from the data considered as valid after the Editing process.

Parameter	From product or updated	Algorithms
Orbit	Updated	DGME-04 (Scharroo and Visser, 1998 [20])
Range	From product and corrected	SPTR2000 (Martini and Féménias, 2000 [16]) + USO drift + current Time Tag Bias
Dry troposphere correction	Updated	Model dry tropospheric correction computed from rectangular grids (new S1 and S2 atmospheric tides are applied)
Inverted Barometer	Updated	Combined atmospheric correction : MOG2D and inverse barometer computed from rectangular grids
Ionosphere correction	Product	BENT model
Sea StatE Bias	Updated	BM3 (Gaspar and Ogor, 1996 [10])
Wet troposphere correction	Updated	this study
Ocean and loading tide	Updated	FES 2004
Terrestrial tide	From product	
Polar tide	Updated	
Mean Sea Surface	Updated	CLS01V1
Orbit Error	Computed	Based on TP adjustement
Mean Sea Level Anomaly	Computed	(where present)

Table 8: *SSH formula*

4.6.3 Results

4.6.3.1 Mapping of the differences between the new and old profiles over the Mediterranean Sea

The 2 mean profiles are compared and presented over the Mediterranean Sea in terms of difference of the number of measurements used for the computation of each mean point (Fig. 32) and difference of height for each mean point (Fig. 33). On average, and as expected for the reasons explained above, each point of the new profile over the open ocean is computed using about 80 points, to be compared to the corresponding value of 60 points for the former profile. Over coastal areas, the new profile usually takes into account more measurements (variable difference) than the old profile. Some exceptions are however noticed in the Agean Sea. Difference on sea level height may be important over coastal areas, frequently reaching 10 to 20 cm (or even more). However, one can also observe smaller but significant difference over the open ocean areas. Finally, it is also interesting to notice that significant differences are observed in the southern coasts of golf of Biscay (6˚W, 44˚N), just in on place where the former profile was suspected to be erroneous.

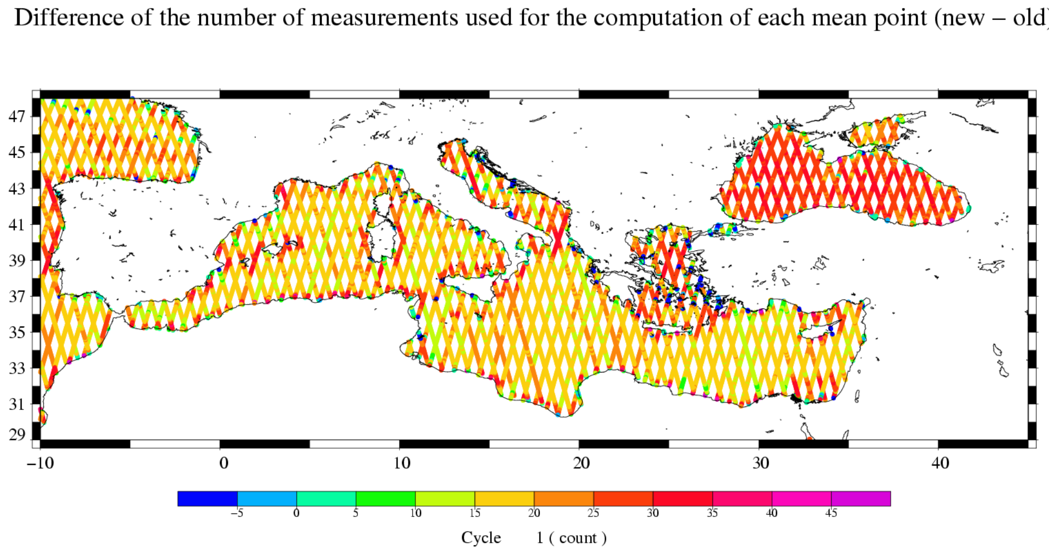

Figure 32: *Difference in the number of measurements used in the computation of each point of the new and old mean profiles over the Mediterranean Sea*

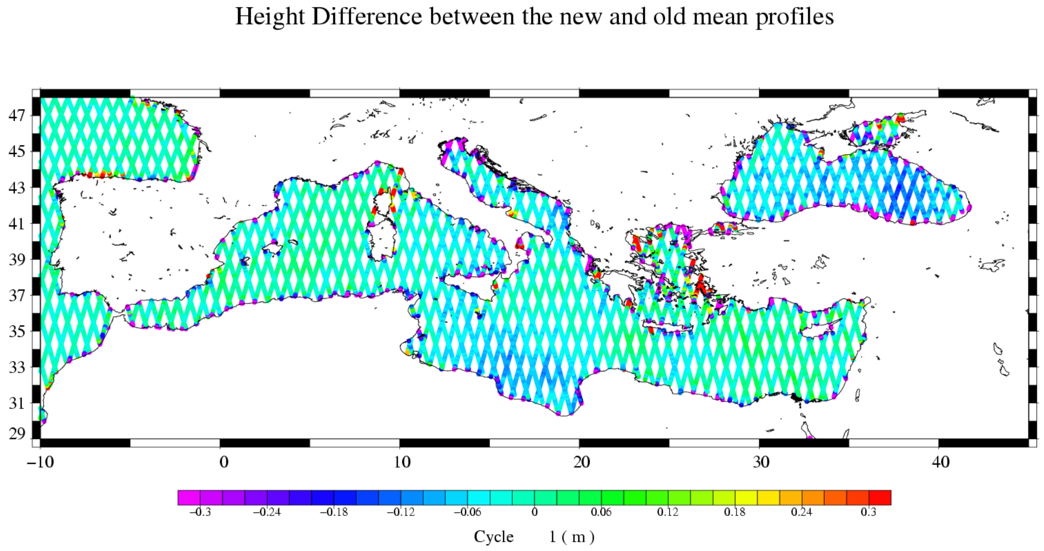

Figure 33: *Height difference between the new and old mean profiles over the Mediterranean Sea*

4.6.3.2 Analysis of track 702 over the Mediterranean Sea

Analysis of track 702 over the Mediterranean Sea Figures 34 and 35 show the number of points and height profiles for track 702. It is obvious that coastal mean points are now computed with a larger number of measurements, at the exception of the northern end of the track in the Adriatic Sea. Moreover, the height profile also appears significantly different near the coasts, with, for example, a variation on each side of Sicily that is opposite in the new and old profiles. The new height signal also appears more realistic, especially around 38˚5 (near the Eolian islands) and when the number of measurements is > 40.

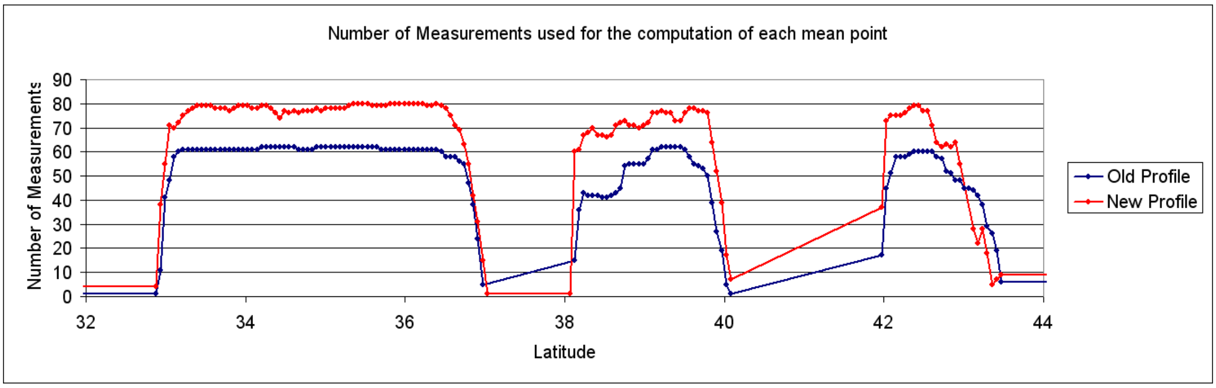

Figure 34: *Number of measurements used in the computation of each point of the old and new mean profiles for pass 702 over the Mediterranean Sea*

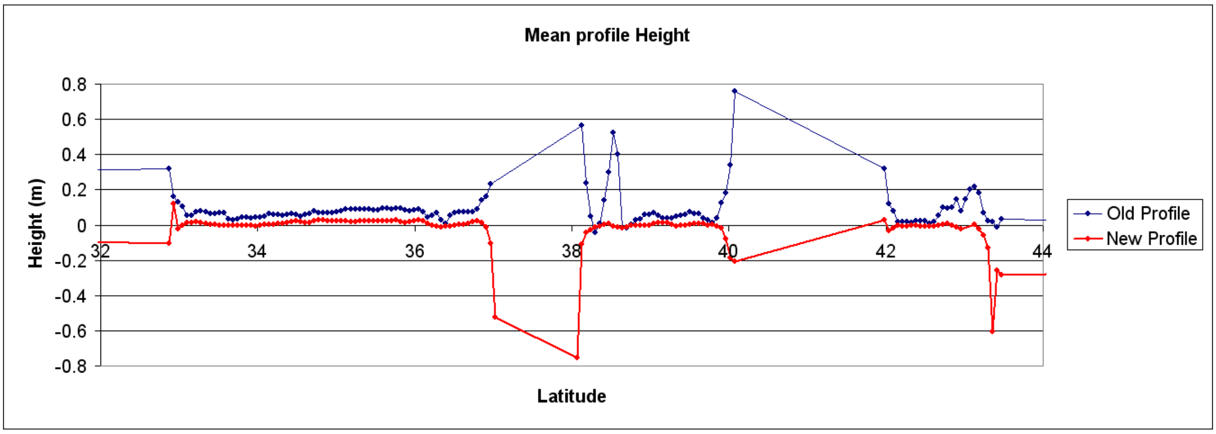

Figure 35: *Height difference at each point of the old and new mean profiles for pass 702 over the Mediterranean Sea*

4.6.4 Conclusion

In the computation of this new mean profile, we used a larger number of cycles as well as the most recent corrections for all parameters. For all these reasons, the new mean appears more realistic and significant discrepancies with the former profile are observed, especially near the coasts, where the mean points are usually computed using a larger number of measurements..

4.7 Conclusion

The objective of the present study was to differentiate and improve the processing of coastal altimetric measurements. The precise localization of each altimetric measurement with respect to the shoreline allowed us to identify several geographical configurations for which a new customized composite wet troposphere correction is computed. This composite correction has been associated to each altimetric measurement, regardless of its distance to the shoreline. Then, we implemented a new parameterization for the Editing process that takes advantage of the developments described in the previous sections. However, it has not been possible to retrieve a significant number of additional coastal measurements, since it appears that the former Editing parameterization is not as restrictive as previously expected. A new mean profile based on ERS2 measurements from cycle 1 to 85 has been computed, and large and significant discrepancies with the former profile are observed. The most important is that the new profile appears more realistic than the former one near the coasts. We hope that regional oceanography studies will benefit from these developments.

5 Conclusion

Despite the failure of the on-board register, the ERS-2 data are still distributed and a work of validation is still needed. The usual validation has been performed during this year and the long-term monitoring is carried on. Moreover, the cross-calibration with Envisat is on-going and minimum of validation is necessary. The statistical results obtained for SWH and SIGMA0 on the data after cycle 85 exhibit a very clear seasonal signal and are consistent considering the geographical coverage. The standard deviation of the mispointing is higher than before June 2003 but the mean of this parameter seems to be steady with a general trend constant from the beginning of cycle 62. The radiometer parameters have been updated with the corrections recommended in the lat annual report and no abnormal behaviour is evidenced from the long-term monitoring. Biases have been computed on ERS-2 TBs and will be useful to apply the future Neural Network algorithm provided for Envisat.
Thanks to the long time series available for ERS-2 from cycles 1 to 85, much work can be done to improve the data set quality in order to use it with Envisat. One goal of this study was to propose a new SSB estimate with up-to-date corrections applied. The methodology of smoothing parameters has been successfully applied to ERS-2, taking into account the particularities of this altimeter. This allowed to propose an estimate from the crossover method, consistent with statistical results, and in-line with the one proposed for Envisat.
Another interesting challenge in data processing is the use of altimetry in coastal regions. The most important drawback is the unavailibility of the radiometer wet troposphere correction in such regions. Until now, there was not any robust method proposed to use the measurements close to the coast. In the present study, a methodology has been developped and performed that takes into account a merging between the model and the radiometer leading to keep the dynamics of the model and to keep a consistency of the correction between the areas where the radiometer correction is available and where the model is used. An example is given in the present study over the Mediterranean sea. With this new correction proposed, it is now possible to propose a special editing available in coastal regions in a way to have as most as possible measurements.
The computation of a mean profile using the up-to-date corrections is carried out and is compared to the one used for the usual products available. Furthermore,

significant improvements can also be expected in coastal areas by refining ERS altimeter data processing and enhancement in these areas. This will lead to more precise coast mean profiles that are essential for applications and studies using past and present altimeter data.

References

[1] Ablain M., 2005, "Jason-1 validation and cross calibration activities",Contract No 03/CNES/1340/00-DSO310 - lot2.C, **CLS.DOS/NT/05.241**

[2] CERSAT, 1996, "Altimeter and Microwave Radiometer ERS Products User Manual", **C2-MUT-A-01-1F, issue 2.2**.

[3] Dorandeu J., F. Mertz and J. Stum, 2000, "Note on ERS-2 Sigma0 variations since January 2000", **CLS.DOS/NT/00.286**. Available at http://www.ifremer.fr/cersat/

[4] Doornbos E., R. Scharro, "Improved ERS and Envisat Precise Orbit determination", Presentation in ERS/Envisat Symposium Saltzburg 2004 The orbit files are available with a latency of 1 to 3 months at http://www.deos.tudelft.nl/ers/precorbs/orbits/.

[5] ECMWF model changes http://www.ecmwf.int/products/data/operational_system/evolution/index.html

[6] Eymard L. and E. Obligis, 1999, "Preliminary report on long-term stability of ERS2/MWR over continental areas"

[7] Eymard L., E. Obligis, N. Tran, February 2003, "ERS2/MWR drift evaluation and correction", **CLS.DOS/NT/03.688**.

[8] Faugere Y., F. Mertz, J. Dorandeu, 2005, "Envisat RA2/MWR ocean data validation and cross-calibration activities." Yearly report. Contract N° 03/CNES/1340/00-DSO310. **CLS.DOS/NT/05.236**. http://www.jason.oceanobs.com/documents/calval/validation_report/en/annual_report_en_2005.pdf

[9] Wessel P., Smith W.H.F., december 1999, GMT, the Generic Mapping Tools, version 3.3.3.

[10] Gaspar P. and F. Ogor, 1996, "Estimation and analysis of the Sea State Bias of the new ERS-1 and ERS-2 altimetric data (OPR V6)", Report of task 2 of IFREMER contract n° 96/2.246.002/C.

[11] Gaspar P., S. Labroue, F. Ogor, G. Lafitte, L. Marchal and M. Rafanel, 2002, "Improving non parametric estimates of the sea state bias in radar altimeter measurements of sea level", *Journal of Atmosphemric and Oceanographic Technology*, **19, 1690-1707**.

[12] see http://iono.jpl.nasa.gov/gim.html

[13] Labroue S. and E. Obligis, September 2001, "Analysis of Neural network retrieval algorithms for the Envisat/MWR", **CLS.DOS/NT/01.378**.

[14] Labroue S., P. Gaspar, J. Dorandeu, O.Z. Zanifé, F. Mertz, P. Vincent, D. Choquet, 2002, "Non parametric estimates of the sea state bias for the Jason-1 radar altimeter", *Marine Geodesy* **Vol 27, 453-482**.

[15] Labroue S., 2005, "RA2 ocean and MWR measurement long term monitoring", 2005 report for WP3, Task 2: SSB estimation for RA2 altimeter, **CLS.DOS/NT/05.200**.

[16] Martini A. and P. Féménias, 2000, "The ERS SPTR2000 Altimetric Range Correction: Results and validation", **ERE-TN-ADQ-GSO-6001**.

[17] Mertz F., J. Dorandeu, N. Tran, S. Labroue, 2004, "ERS-2 OPR data quality assessment. Long-term monitoring - particular investigations", Report of task 2 of IFREMER Contract n° 04/2.210.714, **CLS.DOS/NT/04.277**

[18] Mertz F., Y. Faugère, J. Dorandeu, 2005, "Cycle validation reports", **CLS.DOS/NT/03.702**.

[19] Scharroo R. and P. N. A. M. Visser, 1998, "Precise orbit determination and gravity field improvement for the ERS satellites", *Journal of Geophysical Research*, **103, C4, 8113-8127**.

[20] Scharroo R., J.L. Lillibridge, W.H.F. Smith, and E.J.O. Schrama, 2004, "Cross-Calibration and Long-term Monitoring of the Microwave Radiometers of ERS, TOPEX, GFO, Jason and Envisat", *Marine Geodesy*, **27:279-297**

[21] Tran N. and E. Obligis, December 2003, "Validation of the use of ENVISAT neural algorithms on ERS-2", **CLS.DOS/NT/03.901**.

[22] Tran N.,E. Obligis and L. Eymard, December 2005, "Envisat MWR drift Evaluation and Correction", **CLS.DOS/NT/05.218**

[23] Van Den Bossche M. and O.Z. Zanifé, 2001, "CERSAT2 off-nadire angle evolution. Validation and recommandation note", **CLS.DOS/NT/01.446**.

[24] Van Den Bossche M. and O.Z. Zanifé, 2001, "Impact of the IF filters on altimetry", **CLS.DOS/NT/01.451**.